Pseudomonads associated to salt-stressed plants facilitate stress adaption of soybean through enhanced lignin biosynthesis

Yanfen Zheng[1,3,6]†*, Youqiang Wang[1]†, Ziyan Wang[1]†, Zhe Li[1], Jonathan D. Todd[2,4,5,7], Chen Meng[1], Shutian Hua[1], Xiaona Sui[1], Qingchen Rui[1], Siqi Ma[1], Yiqiang Li[1,3,6*], Jiwen Liu[2*], Donglin Zhao[1,3,6*], Chengsheng Zhang[1,3,6*]

[1]Tobacco Research Institute, Chinese Academy of Agricultural Sciences, Qingdao, 266101, China

[2]MOE Key Laboratory of Evolution and Marine Biodiversity, Frontiers Science Center for Deep Ocean Multispheres and Earth System, and College of Marine Life Sciences, Ocean University of China, Qingdao, 266003, China

[3]National Center of Technology Innovation for Comprehensive Utilization of Saline-Alkali Land, Dongying, 257300, China

[4]School of Biological Sciences, University of East Anglia, Norwich Research Park, Norwich NR4 7TJ, UK

[5]Centre for Microbial Interactions, Norwich Research Park, Norwich, NR4 7TJ, UK

[6]Qingdao Center of Technology Innovation for Microbial Germplasm, and the Key Laboratory of Bio-resources Evaluation and Utilization in Saline-alkali Soil, Qingdao, 266101, China

[7]Quadram Institute Bioscience, Norwich Research Park, Norwich, Norfolk NR4 7UQ, UK.

[*]Correspondence: zhangchengsheng@caas.cn; zhaodonglin@caas.cn; liujiwen@ouc.edu.cn; liyiqiang@caas.cn; zhengyanfen@caas.cn

†These authors contributed equally: Yanfen Zheng, Youqiang Wang, Ziyan Wang

Short title: Pseudomonads facilitate soybean stress adaption

Teaser: Pseudomonads enhance soybean salt tolerance via plant lignin biosynthesis rather than the canonical mechanism of Na^+ homeostasis.

Abstract

Root-associated microbiota play a critical role in plant tolerance to salt stress. However, the conservation of beneficial interactions across diverse crops and soils, and the underlying mechanisms, remain unclear. Here, we show that pseudomonads were consistently enriched in salt stressed plant roots across multiple soil types and most crop species. Comparative genomics revealed that these pseudomonads harbored unique genomic signatures associated with high salinity tolerance, such as Na^+ transporters. Pseudomonad isolates from salt-stressed plants robustly colonized soybean roots, and significantly improved salt tolerance under both greenhouse and field conditions. Importantly, pseudomonads-dependent plant salt stress tolerance was mediated though plant lignin biosynthesis stimulation rather than the canonical mechanism of Na^+ homeostasis. Overexpression of the key plant lignin biosynthesis genes, including *GmCAD*, *GmCOMT* and *Gm4CL*, significantly enhanced soybean growth under salt stress. Furthermore, mutant plants deficient in lignin biosynthesis no longer showed pseudomonads-induced salt tolerance. Collectively, our findings reveal a previously unrecognized microbial-mediated pathway that enhances plant resilience to salt stress.

Key words: Root microbiota; Pseudomonads; Salt stress; Lignin biosynthesis

Introduction

Soil salinization is a major global threat to soil fertility (*1*), biodiversity (*2*) and crop yield (*3*). Through climate change, the extent and persistence of salinization are predicted to exceed those observed in recent decades (4), posing a serious threat to global food security. Numerous studies on salt-tolerant plants have uncovered a range of adaptive strategies to cope with salt stress, such as ion homeostasis, accumulation of compatible solutes, and hormonal regulation (*5, 6*). Soil microbiota are key drivers of plant productivity and ecosystem function, and they also play a critical role in enhancing plant survival under saline conditions (*7, 8*). Therefore, understanding the interactions between soil microorganisms and plants is essential for improving crop performance in saline-affected soils and for supporting sustainable agriculture.

The "cry for help" hypothesis has recently been proposed to describe a strategy whereby plants under biotic or abiotic stresses actively secret specific compounds to recruit beneficial microorganisms that enhance stress adaptation (*9, 10*). Increasing evidence suggests that conserved microbial recruitment patterns may occur across diverse plant species in response to specific stresses. For example, *Pseudomonas* are frequently enriched in rhizospheres to resist pathogen attacks (*11, 12*). Under nitrogen deprivation, *Massilia* have been reported to be recruited across diverse plant species to improve nitrogen acquisition and host performance (*13-15*). Similarly, under drought stress, *Streptomyces* are consistently enriched across diverse plants and soil types (*16-18*). In a recent study, Zheng et al. (*19*) reported a significant enrichment of *Pseudomonas* within the salt-stressed roots of wild soybean (*Glycine soja*), and that such *Pseudomonas* isolates enhanced plant resilience to salt stress. Based on these observations, we hypothesize that a conserved plant-microbe interaction mechanism may exist for salt stress tolerance, likely mediated by a common group of beneficial bacteria.

The microbial driven mechanisms for enhancing plant salt tolerance are proposed to

include regulation of ion homeostasis, osmoprotectant synthesis and reactive oxygen species (ROS) scavenging (*20-22*). Rhizospheric pseudomonads are one of the most widely recognized microorganisms to benefit plants (*23*), and growing evidence shows that they enhance plant resistance to both abiotic and biotic stresses by producing plant growth regulators, such as indole-3-acetic acid (IAA), siderophores, and antimicrobial compounds, as well as by inducing systemic resistance in plants (*24-26*). Recent studies have reported that some pseudomonads alleviate plant salt stress by moderating antioxidant enzyme activities, proline accumulation and the Na^+/K^+ ratio (*27, 28*). Despite widespread claims regarding the physiological efficacy of pseudomonads inoculation (*29*), the molecular mechanisms underlying its role in enhancing plant salt tolerance remains limited.

This study hypothesized that salt stress enhances root-associated *Pseudomonas* populations across diverse plant species and soil types. To test this hypothesis, we employed genome-resolved metagenomics to investigate the rhizosphere microbiome shifts associated with salt stress of wild soybean. We included multiple soil types spanning a latitudinal gradient across China, classified as alkaline or acidic, as well as diverse plant species, including the key crops maize (*Zea mays*) and sorghum (*Sorghum bicolor*), to determine whether the observed microbial response is species-specific or broadly conserved. Functional differences between salt-enriched and salt-depleted microbial taxa were identified by comparative genomics, to uncover potential genetic adaptations underlying their stress-associated proliferation. Moreover, we conducted a series of genetic, transcriptomic, and inoculation experiments to elucidate the mechanisms by which *Pseudomonas* enhance plant salt tolerance.

Results

Identification of salt-enriched taxa from metagenome-assembled genome (MAG) analysis of wild soybean rhizosphere soils

To determine how salt stress shapes the rhizosphere microbiome, we revisited the

metagenomic data from rhizosphere soils of salt-stressed and control wild soybean generated in Zheng et al. (*19*). A total of ~264 Gb high-quality data was retrieved from 16 rhizosphere soils of wild soybean treated with salt stress (100 mM, 200 mM and 300 mM NaCl) or without (0 mM NaCl; control). We extended the previous analysis, which focused on functional genes from the non-redundant gene set (*19*), by recovering MAGs to better resolve the salt stress induced shift in taxonomy at the genomic level. Binning of assembled contigs from these metagenomic data resulted in 164 non-redundant MAGs (completeness ≥ 50% and contamination ≤ 10%), including 157 bacterial MAGs and 7 archaeal MAGs (table S1). The most dominant phyla were *Pseudomonadota* ($n = 48$), *Actinomycetota* ($n = 32$), and *Acidobacteriota* ($n = 20$) (Fig. 1A). Consistent with the 16S rRNA gene barcoding analysis (*19*), the MAG dataset also demonstrated a strong enrichment of *Pseudomonas* and a large decrease in the relative abundance of *Acidovorax* in the rhizosphere community under all levels of salt stress, as compared to the control (Fig. 1B).

To determine whether salt-enriched MAGs exhibited distinct functional profiles compared to salt-depleted MAGs, we identified 35 out of 164 MAGs with significant abundance changes between control and salt treatments, including 21 salt-enriched and 14 salt-depleted MAGs (Fig. 1 and fig. S1). Functional annotation using the Clusters of Orthologous Groups (COG) database revealed no significant differences between the enriched and depleted groups [Analysis of similarities (ANOSIM): $R = 0.089$, $P = 0.053$] (Fig. 1C and table S2). Using Kyoto Encyclopedia of Genes and Genomes (KEGG) annotations, we further assessed the plant growth-promoting (PGP) potential of MAGs and similarly found no statistically significant differences (ANOSIM: $R = 0.046$, $P = 0.172$; Fig. 1D and table S3). These results suggested that salt-enriched MAGs lacked common functional signatures, at least within the tested databases. Note, previously Zheng et al. observed a marked enrichment of genes associated with cell motility (COG category N) in salt-treated samples (*19*). This enrichment could largely be attributed to the high number of motility-related genes in *Pseudomonas* MAG (e.g., bin149; Fig. 1E).

Together, these findings provided genomic-level support for the previously observed enrichment of *Pseudomonas* in salt-stressed root systems (*19*). In contrast, *Acidovorax* was identified as the most strongly depleted taxon under salt stress.

Salt-mediated *Pseudomonas* enrichment is conserved across diverse soils

To examine if plant enrichment of *Pseudomonas* under salt stress was conserved across different soils, we collected experimental soils from 10 different fields in China spanning a latitudinal range of 12 degrees and different pH gradients (Fig. 2A, and tables S4 and S5). Wild soybean seedlings were grown in the above soils for 10 days and then treated with 300 mM NaCl or sterile water (control) for two weeks in a green greenhouse (fig. S2). 16S rRNA gene barcoding analysis showed that salt stress significantly decreased the α-diversity of root microbiota in alkaline soils, while a similar but non-significant trend was observed in acidic soils (Fig. 2B). For β-diversity, microbial communities significantly differed between wild soybean grown in alkaline and acidic soils. Moreover, salt stress exerted a stronger influence on the microbial communities associated to plants grown in acidic soils compared to alkaline soils (Fig. 2C).

To determine how salt stress affected bacterial recruitment by wild soybean across different soils, we first analyzed the compositional profiles at the order level. *Burkholderiales* and *Rhizobiales* were dominant across both control and salt-treated samples, regardless of alkaline or acidic soils (fig. S3). Intriguingly, salt stress significantly increased the relative abundance of *Pseudomonadales* by 9.6-fold in the wild soybean grown in alkaline soils (Student's *t* test, $P = 9.5 \times 10^{-7}$; from 1.4% of control to 13.6% of salt-treated samples), whereas no significant change was observed in acidic soils (Student's *t* test, $P = 0.71$). Of the top 10 abundant genera, *Pseudomonas* exhibited the most pronounced positive response to salt stress (fig. S4), with fold increases ranging from 3.9 to 96.9 in alkaline soils (Fig. 2D). Note, a salt-induced enrichment of *Pseudomonas* was also observed in acidic soils (Fig. 2E), albeit with

modest increases ranging from 0.7 to 4.0-fold. Further analysis of salt-enriched operational taxonomic units (OTUs) in alkaline soils revealed *Pseudomonas* OTU12019 as the most significantly enriched taxon in salt-treated wild soybean roots [Student's *t* test, $P = 2.1 \times 10^{-6}$; $\log_2$(fold change) = 5.2], with a weaker but still significant enrichment in acidic soils [Student's *t* test, $P = 0.01$; $\log_2$(fold change) = 1.7] (Fig. 2F). Consistent with the MAG-based observations (Fig. 1), there was also a significant depletion of *Acidovorax* in the salt-treated roots, both in alkaline and acidic soils (Fig. 2E). Combined these data implied that *Pseudomonas* had a competitive advantage over other root-associated bacteria under salt stress conditions, which was conserved across distinct soils, but more pronounced in alkaline soils.

Salt-mediated *Pseudomonas* enrichment is conserved across plant hosts

To determine if salt stress induced *Pseudomonas* enrichment is conserved across different plants, six common crops (table S5), including maize (*Zea mays*), sorghum (*Sorghum bicolor*), rice (*Oryza sativa*), wheat (*Triticum aestivum*), rapeseed (*Brassica napus*) and tomato (*Solanum lycopersicum*) were planted and studied in alkaline soils. Ten-day-old plants were subjected to 200 mM NaCl or sterile water (control), and root samples were collected after two weeks. For all plant species, salt stress significantly decreased bacterial α-diversity (Shannon index; fig. S5) and induced shifts in community compositions (Fig. 3A and fig. S6). Consistent with observations in wild soybean, the abundance of *Acidovorax* dramatically decreased in the rhizosphere of all tested salt stressed plant species (Fig. 3B). Similarly, *Pseudomonas* were the most strongly enriched taxa in the salt stressed maize, sorghum, rapeseed, and tomato roots with their relative abundance increasing from 1.42%-21.56% in control to 22.84%-41.12% in salt stressed samples (Fig. 3C). However, *Pseudomonas* were not enriched in the salt stressed roots of rice and wheat (Fig. 3B). These data implied that salt stress induced enrichment of *Pseudomonas* was conserved across many diverse cropped plants, but that this was not a universal phenomenon.

194 ***Pseudomonas* harbor versatile genetic capabilities for salt tolerance**

195 With the contrasting responses of *Pseudomonas* and *Acidovorax* to salt stress in most
196 plants, we hypothesized they had contrasting salt tolerance and genetic architectures for
197 salt stress resistance. To test this hypothesis, we reviewed published data on the salt
198 tolerance of their type strains and found that *Pseudomonas* strains tolerated NaCl
199 concentrations up to 4.9%, whereas most *Acidovorax* species exhibited limited growth
200 at around 1.5% NaCl (Fig. 4A and table S6). Next, comparative genomics was
201 conducted on 359 reference *Pseudomonas* genomes and 128 *Acidovorax* genomes
202 publicly available in the NCBI database (table S7 and S8). Compiling the geographical
203 source of each genome showed that *Pseudomonas* were potentially distributed across
204 more diverse habitats than *Acidovorax* (Fig. 4, B and C), although this pattern may be
205 influenced by unequal genome number for the two genera. With a focus on genes
206 associated with PGP traits and salt stress alleviation, functional gene annotation against
207 the KEGG database revealed that while PGP [e.g., 1-aminocyclopropane-1-carboxylate
208 (ACC) deaminase, IAA biosynthesis, and phosphatases] related genes showed some
209 variability between *Pseudomonas* and *Acidovorax*, the most striking differences were
210 observed in stress-related gene contents. Compared to *Acidovorax*, *Pseudomonas*
211 harbored far more genes involved in antioxidation, betaine synthesis and transport, and
212 Na^+ transport (Fig. 4D).
213
214 Using antiSMASH, 3,873 and 616 putative biosynthetic gene clusters (BGCs) were
215 identified in *Pseudomonas* and *Acidovorax*, respectively. On average, the number of
216 BGCs per genome was two-fold higher in *Pseudomonas* than in *Acidovorax* (fig. S7A),
217 suggesting that *Pseudomonas* species possess greater genetic potential for secondary
218 metabolite biosynthesis. Moreover, these two genera displayed different BGC profiles.
219 The predicted product classes of *Pseudomonas* mainly comprised non-ribosomal
220 peptides (NRPS, 32.5%), ribosomally synthesized and post-translationally modified
221 peptides (RiPP, 13.1%), redox-cofactor (9.2%), and N-acetylglutaminylglutamine
222 amide (NAGGN, 8.6%), whilst *Acidovorax* comprised terpenes (23.5%), RiPP (19.5%),

betalactones (15.7%), and NRPS (14.4%) (fig. S7, B and C). Strikingly, the potential secondary metabolites related to salt tolerance, including NRPS, siderophore, NAGGN, and ectoine, were found to be far more prevalent in *Pseudomonas* compared to *Acidovorax* species (Fig. 4C). In particular, the compatible solute NAGGN was ubiquitously present across nearly all *Pseudomonas* species, whereas it was not predicted in any *Acidovorax* species. Given some *Pseudomonas* and *Acidovorax* genome assemblies were incomplete, we reanalyzed salt tolerance–related pathways using only complete genomes to assess whether genome completeness impacted our estimation of these functions. The results were consistent with those from the full genome datasets (fig. S8), indicating that the observed differences between the two genera are robust and not affected by genome assembly level.

Since NAGGN synthesis potential was the most conspicuous predicted metabolic difference between *Pseudomonas* and *Acidovorax*, we hypothesized that it played a key role in salt tolerance in *Pseudomonas*. To test this, two representative *Pseudomonas* strains, *P. stutzeri* XN05-1 and *P. frederiksbergensis* YE17, previously isolated from salt-treated wild soybean roots in Zheng et al. (*19*), were selected for further experiments. AntiSMASH analysis revealed that both XN05-1 and YE17 strains harbored the NAGGN biosynthetic gene cluster (fig. S9). This cluster comprised three NAGGN synthesis genes encoding N-acetylglutaminylglutamine amidotransferase, N-acetylglutaminylglutamine synthetase, and peptidase (designated as *nbsABC* in this study; Fig. 4E and table S9). Deletion of *nbsABC* in strain XN05-1 severely impaired growth compared to the wild-type strain in media containing 3-7% NaCl (w/v), and strain YE17 exhibited markedly reduced growth under 3-5% NaCl (w/v) conditions (Fig. 4F). These results suggest that NAGGN biosynthesis represents one of the key strategies used by *Pseudomonas* to tolerate high salinity, which may contribute to their enrichment in plant roots under salt stress.

Pseudomonas alleviate soybean salt stress via a non-canonical salt-tolerance

mechanism

The consistent enrichment of salt-tolerant *Pseudomonas* in roots of many plant species under salt stress made it an ideal model system to examine their potential interaction and benefits to salt-stressed plants. Soybean (*Glycine max*), an economically important crop that has evolved from wild soybean, was utilized as the model plant. To determine whether *Pseudomonas* could colonize soybean roots, *Pseudomonas* strains XN05-1 and YE17 were inoculated onto soybean seedlings, and their root colonization was examined using scanning electron microscopy. Both *Pseudomonas* strains robustly adhered to the root surface (Fig. 5A). To quantify colonization dynamics under salt stress (50 mM NaCl), *Pseudomonas* strains were genetically tagged with green fluorescent protein (GFP), which showed no detectable effects on motility and only a minor effect on growth kinetics (fig. S10). The fluorescence intensity revealed both strains exhibited a twofold increase in root colonization under salt stress compared to control conditions (Fig. 5, B and C). Colony forming units (CFU) enumeration further confirmed effective root colonization, with strains XN05-1 and YE17 reaching densities of 1.78×10^6 and 1.12×10^6 CFU per gram of fresh root under salt stress, respectively. Consistent with their enhanced colonization, salt-stressed soybean plants inoculated with either XN05-1 or YE17 exhibited significant growth promotion, particularly in root growth and development (fig. S11, A and B). Morphological observations further confirmed that both *Pseudomonas* strains significantly promoted root elongation and lateral root formation under salt stress (Fig. 5, C to E, and fig. S11C).

To elucidate the molecular mechanisms underlying the enhancement of salt tolerance in soybean by *Pseudomonas*, RNA-seq analysis was performed on the roots of soybean inoculated and un-inoculated (mock) with strains XN05-1 and YE17. Compared to the control condition, the inoculated soybean roots exhibited pronounced transcriptional reprogramming under salt stress conditions (300 mM NaCl) (Fig. 5, G and H, and fig. S12, A and B). Specifically, inoculation with strains XN05-1 and YE17 under salt stress resulted in 5972 (up: 1628, down: 4344) and 928 (up: 381, down: 547) differentially

expressed genes (DEGs), respectively. In contrast, under control condition, only 177 and 149 DEGs were identified for strains XN05-1 and YE17, respectively (table S10). Given that Na^+ toxicity will directly impair root growth, we hypothesized that the observed growth promotion by *Pseudomonas* involves Na^+ homeostasis regulation. Unexpectedly, Na^+ and K^+ transporter genes (including members of the *CHX*, *NHX*, and *HKT* families) were not differentially expressed in response to either XN05-1 or YE17 inoculation (Fig. 5H and table S11). Consistent with this, ion content analysis revealed no significant differences in root Na^+ or K^+ contents between inoculated and mock-treated plants under either salt or control conditions (Fig. 5, I and J). Taken together, these data revealed that *Pseudomonas* strains XN05-1 and YE17 mitigated salt stress in soybean through a non-canonical salt-tolerance mechanism.

Pseudomonas **improve soybean salt tolerance by enhancing root lignin biosynthesis**

To reveal the mechanisms underlying *Pseudomonas*-mediated salt tolerance, we performed KEGG enrichment analysis of the soybean root transcriptomes. A phenylpropanoid biosynthesis pathway was significantly enriched in roots inoculated with either XN05-1 or YE17 under salt stress (Fig. 6A), but not under control condition (fig. S12, C and D), indicating that *Pseudomonas*-mediated activation of this metabolic pathway was specific to salt stress. In the phenylpropanoid biosynthesis pathway, the gene *Glyma.01G021000* was strongly induced by strains XN05-1 and YE17. This gene (named *GmCAD*) encodes cinnamyl alcohol dehydrogenase, an enzyme that plays a critical role in lignin synthesis. Strikingly, several other lignin-associated genes, including *Gm4CL*, *GmCCR*, *GmCOMT*, and *GmPOX*, were also upregulated in the roots of soybean inoculated with *Pseudomonas* strains (Fig. 6B). Thus, we hypothesized that *Pseudomonas* may activate lignin biosynthesis in the roots to enhance soybean salt tolerance. To test this hypothesis, plant lignin content was quantified following *Pseudomonas* inoculation. Under salt stress, lignin levels in roots increased by 35.2% and 30.3% upon inoculation with strains XN05-1 and YE17, respectively,

whereas no significant changes were observed under the control condition (Fig. 6C). Phloroglucinol staining also showed enhanced lignin deposition (red and purple coloration) in the root cell walls of inoculated plants (Fig. 6D). These results supported the notion that *Pseudomonas*-induced lignin biosynthesis was specifically triggered by salt stress.

To further validate the role of lignin biosynthesis in soybean salt tolerance, plant lines over-expressing *GmCAD*, *Gm4CL* and *GmCOMT* (*OE-GmCAD*, *OE-Gm4CL* and *OE-GmCOMT*) were generated using a transgenic hairy root system (fig. S13). Compared to the wild-type (WT), all over-expression lines exhibited enhanced salt tolerance, as evidenced by a marked reduction in leaf chlorosis symptoms (Fig. 6E). In addition, root elongation was significantly improved in *OE-GmCAD*, *OE-Gm4CL*, and *OE-GmCOMT* plants compared to WT under both control and salt stress conditions (Fig. 6F). This improvement in root elongation was more pronounced under salt stress, showing a 3.3 to 13.4-fold increase compared to the 2.5 to 3.4-fold improvement under control conditions, suggesting that overexpression of lignin biosynthesis genes conferred a salt stress-specific advantage. Supporting this conclusion, soybean plants with disrupted lignin biosynthesis genes no longer displayed *Pseudomonas*-induced salt tolerance (Fig. 6G), confirming lignin biosynthesis as a critical mechanism underlying this beneficial interaction.

Field trials are essential for evaluating microbial inoculants under real-world conditions. A field experiment conducted in naturally saline soil (salinity of 0.42%) showed that soybean plants inoculated with *Pseudomonas* strains exhibited superior growth performance relative to uninoculated controls (Fig. 6H). Specifically, inoculation with *Pseudomonas* led to notable increases in root biomass, nodule number, and pod number compared to non-inoculated plants (Fig. 6, I to K). These findings indicated that the application of *Pseudomonas* strains enriched from salt-stressed plants offers a promising strategy for improving crop performance in saline agriculture. Collectively,

our findings establish a mechanistic link between *Pseudomonas* symbiosis and enhanced salt tolerance in soybean, wherein root-associated *Pseudomonas* activate the host's lignin biosynthesis, leading to root architectural modifications that contribute to improved stress resilience (Fig. 7). However, further work is needed to establish exactly how *Pseudomonas* enhanced plant lignin gene expression, if this mechanism is conserved in the other plants for which pseudomonads were enriched by salt stress.

Discussion

Although plants have evolved diverse adaptive mechanisms to cope with biotic and abiotic stresses in nature, they still rely on their microbial partners to bolster survival and provide additional protection against these stresses (*30-32*). In this study, genome-wide insights were provided into shifts of root microbiota composition of wild soybean under salt stress. The observed enrichment and depletion of specific taxa, exemplified by *Pseudomonas* and *Acidovorax*, respectively (Fig. 1), supported the notion that abiotic stresses significantly influenced the assembly of plant-associated microbiomes (*13, 33*). Extending this, we further found that the salt-induced enrichment of *Pseudomonas* was a highly conserved phenomenon across most tested diverse plant species and soil backgrounds (Figs. 2 and 3), indicating its selective advantage of salt-adaption and beneficial roles in stress alleviation (Fig. 4). We experimentally confirmed that *Pseudomonas* enhanced soybean salt tolerance through a lignin-mediated mechanism, in contrast to the widely recognized mechanism of ion homeostasis (Fig. 5 and 6). This finding highlights the potential of harnessing root-associated microbiota to improve crop resilience under saline conditions.

Different plant species possess unique root architectures, exudation profiles, and abiotic stress tolerance, all of which have been shown to shape symbiotic microbial communities (*34, 35*). Unexpectedly, most crops examined here exhibited a conserved pattern of *Pseudomonas* enrichment. This finding aligns with previous reports of salt-induced *Pseudomonas* enrichment in both salt-sensitive and salt-tolerant plants within

the family Curcurbitaceae, such as *Cucumis sativus*, *Cucurbita ficifolia*, and *Lagenaria siceraria* (*36*). Together with our prior demonstration of this phenomenon in salt-stressed wild and domesticated soybean (*19*), these results support the conclusion that *Pseudomonas* enrichment is a broadly conserved response to salt stress across diverse plant species, despite notable exceptions in rice and wheat. These exceptions might be caused by either lineage-specific host selection mechanisms or differential host genetic factors that influenced microbiome recruitment. To further elucidate the interplay between salt stress and *Pseudomonas* enrichment in plants, future research should determine the salt stress threshold needed for *Pseudomonas* enrichment and assess whether this relationship follows a linear pattern or exhibits greater complexity.

Pseudomonas species exhibit significant plant-beneficial traits, notably the production of diverse bioactive metabolites (*25*) and other compounds that help plants withstand biotic (*37, 38*) and abiotic stresses (*39*). These may explain its widespread occurrence in salt-stressed plants. Members of *Pseudomonas* have been shown to synthesize the compatible solute NAGGN in response to osmotic stress (*40-42*). Consistent with this, comparative genomic analysis revealed that the NAGGN biosynthetic gene cluster is widely present across nearly all *Pseudomonas* species (Fig. 4C). Disruption of the NAGGN biosynthetic pathway significantly impaired the growth of *Pseudomonas* strains under saline conditions (Fig. 4E). This osmoprotective mechanism may contribute to the observed enrichment of *Pseudomonas* in salt stressed root microbiomes. Given the conserved nature of this enrichment, we propose the *Pseudomonas* genus as a promising model system for investigating plant–microbe interactions under saline conditions.

Microbe-mediated strategies for plant adaptation to salt stress have gained wide recognition, with core mechanisms involving the maintenance of ion homeostasis, scavenging of reactive oxygen species (ROS), and activation of stress response signaling pathways (*20, 21, 43*). Among these, the regulation of Na^+ homeostasis is

regarded as a key mechanism by which plants adapt to salt-stress conditions (*44*). However, our RNA-seq analysis revealed that *Pseudomonas* did not directly activate genes or pathways related to Na^+ transport, such as *CHX* and *NHX* genes (Fig. 5D). Intriguingly, we found that *Pseudomonas* significantly induced enrichment of the phenylpropanoid metabolic pathway, with multiple lignin biosynthesis-related genes (*GmCAD*, *Gm4CL*, and *GmCOMT*) exhibiting marked differential expression (Fig. 6, A and B). This led to elevated root lignin content and evident lignin deposition in the cell wall (Fig. 6, C and D). Lignin is a major component of the cell wall and plays a critical role in enhancing cell wall mechanical strength and structural stability (*45*). It has been demonstrated that increasing lignin content can significantly enhance plant salt tolerance and growth performance (*46, 47*). For instance, in tomato, overexpression of *SlCOMT2* promoted both plant growth and salt tolerance (*48*). Notably, *Pseudomonas*-induced lignin biosynthesis was mainly observed under salt stress, indicating that stress condition was essential for the activation of this pathway by *Pseudomonas*. Our previous work has identified purines as key chemical signals mediating the enrichment of *Pseudomonas* under salt stress (*19*). These findings together suggested a coordinated interaction, in which salt stress first promoted the secretion of root-derived purines to recruit *Pseudomonas*. In turn, *Pseudomonas* functioned as a specific signal that activated the host lignin biosynthetic pathway, thereby enhancing plant stress tolerance. However, future studies are needed to elucidate how *Pseudomonas* activates these plant lignin biosynthetic genes.

Collectively, our study provides the most comprehensive investigation to date of how salt stress shapes root bacterial communities across diverse soil types and plant species. The discovery of the conserved enrichment of *Pseudomonas* in salt-stressed plant root underwrites its ecological significance as a key stress-alleviating taxon. We further establish *Pseudomonas* as a model system for investigating plant-microbe interactions under salt stress, and evidence that specific strains enhance soybean salt tolerance through a lignin-dependent mechanism, revealing a previously unrecognized microbial

strategy for modulating host salt resilience. These findings fill key knowledge gaps in understanding how environmental stress reconfigures the plant microbiome, and identify lignin biosynthesis as a promising target for breeding salt-tolerant crops and screening of beneficial microbes.

Materials & Methods

Metagenomic sequencing and binning

As described in Zheng et al. (*19*), 10-day-old wild soybeans were treated with 100, 200 or 300 mM NaCl (60 mL per pot, applied as 20 mL per day for three consecutive days), with sterile water as the control. Rhizosphere soils were collected at 14 days after the salt treatment and six plants per pot were combined to generate one composite sample. Each treatment had four biological replicates.

Genomic DNA of rhizosphere soil was extracted using the FastDNA® Spin Kit for Soil (MP Biomedicals) following the manufacturer's protocol. Libraries were prepared without amplification and sequenced on the Illumina HiSeq X-Ten platform at the Majorbio Bio-Pharm Technology. After removing adapter and reads containing low quality bases or 10% of undefined bases, ~264 Gb high-quality data was generated from 16 samples, as reported previously in Zheng et al. (*19*). This study focused on MAGs to better resolve the salt stress induced shift in taxonomy at the genomic level. Briefly, MetaWRAP v1.3.2 (*49*) was used for assembly and genomic binning. Two groups of co-assemblies were performed using MegaHit v1.1.3 (*50*) through the "assembly module" in MetaWRAP, with one including only the control samples, and the other including all salt treatment samples. Assembled contigs were binned using MetaBAT2 v2.12.1(*51*), MaxBin2 v2.2.6 (*52*), and CONCOCT v1.0.0 (*53*) integrated within the MetaWRAP pipeline. The retrieved MAGs were refined using the "bin_refinement" module with the options -c 50 and -x 10. All bins were subsequently dereplicated using dRep v2.2.3 (*54*) with the following parameters: -sa 0.99, -nc 0.1. Finally, we obtained 164 non-redundant MAGs for downstream analyses.

MAG analyses

The completeness and contamination of MAGs were evaluated by CheckM v1.0.12 (*55*). Taxonomic classifications of MAGs was performed using the GTDB-Tk v2.4.0 (*56*) with 'gtdbtk classify_wf' against the GTDB database release 220 (*57*). Genes were predicted using Prodigal v2.6.3 (*58*) and annotated with Prokka. Additional annotations were performed by aligning genes to the EggNOG 5.0 (*59*) database using eggNOG-mapper v2.1.12 (*60*). The KEGG and COG term annotation results for each gene were extracted from the output of eggNOG-mapper. Relative abundance of the MAGs in each sample was calculated by CoverM v0.7.0 (available at https://github.com/wwood/CoverM), with the parameter --min-read-percent-identity 0.95 and --min-read-aligned-percent 0.5. A phylogenetic tree of 164 MAGs was constructed using PhyloPhlAn 3.0 (*61*) based on concatenated alignments of up to 400 ubiquitously conserved proteins, and then visualized using iTOL (https://itol.embl.de/) (*62*).

Salt-induced *Pseudomonas* enrichment across different soils and hosts

For experiment 1, we aimed to characterize whether salt-induced *Pseudomonas* enrichment is conserved across different soil types. Bulk soils at a depth of 0-10 cm were collected from 10 geographically distinct fields across China, spanning a latitudinal range of 12 degrees (table S4). Soil pH was determined in a mixture with 1:5 ratio of soil: water using pH meter (Thermo Orion Star A111, Thermo Fisher, Germany). We grew wild soybean plants using these soils under controlled conditions. Briefly, wild soybean seeds were surface sterilized with 0.15% mercuric chloride for 10 min and thoroughly washed with sterile water. Thereafter, the seeds were germinated in Petri dishes with sterile water in the dark at 25°C for 2 days. Seedlings were transferred to plastic pots containing 200 g of field soil, and incubated in a growth chamber at 25°C under a 16/8 h light/dark photoperiod (light intensity, 200 μmol m^{-2} s^{-1}) and 65% relative humidity. Plants were regularly watered with sterile water as needed. After 10

days of growth in pots, wild soybean plants were treated with 300 mM NaCl (60 mL per pot, applied as 20 mL per day for three consecutive days), while control plants received 60 mL of sterile water applied in the same manner. The experiment was performed with five biological replicates (table S5).

For experiment 2, we aimed to explore whether salt-induced *Pseudomonas* enrichment was conserved across different plant species. The plant materials used in this study included maize (*Zea mays*, cv. Zhengdan 958), sorghum (*Sorghum bicolor*, cv. Kangsi), rice (*Oryza sativa*, cv. Zhenghan No.10), wheat (*Triticum aestivum*, cv. Jimai 22), rapeseed (*Brassica napus*, cv. Zhongshuang 11) and tomato (*Solanum lycopersicum*, cv. Zhongshu No. 4), all of which are important crops. All seeds were surface sterilized with 0.15% mercuric chloride for 10 min and thoroughly washed with sterile water. They were germinated in Petri dishes with sterile water in the dark at 25°C for 2-3 days. Seedlings were transferred to plastic pots, each containing 200 g of the same soil used in our previous study (*19*). Plants were regularly watered with sterile water as needed. Since these crops are not salt-tolerant plants, 200 mM NaCl (60 mL per pot, applied as 20 mL per day for three consecutive days) were imposed on 10-day-old plants. Control plants received 60 mL of sterile water applied in the same manner. The experiment was performed with five biological replicates (table S5).

Sampling, DNA extraction and 16S rRNA gene barcoding

Since salt-induced *Pseudomonas* enrichment is more pronounced in root samples than in rhizosphere soil as described by Zheng et al. (*19*), we focused on root samples to further evaluate whether this pattern is conserved across soils and plant species. Root samples were collected at 14 days after the salt treatment. All plants within each pot (six for wild soybean, wheat and rice; four for maize, sorghum, rapeseed and tomato) were combined to generate one composite sample. To collect root samples, root-adhered soil was first removed by gently washing under running water. Roots were then further washed, sonicated and frozen at -80 ℃ until DNA extraction. Due to failure of

DNA extraction or 16S rRNA gene amplification, several treatments included less than five but more than three biological replicates. The summary of sampling information is shown in table S5.

Genomic DNA was extracted using the FastDNA® Spin Kit for Soil (MP Biomedicals) according to the manufacturer's protocol. The concentration of extracted DNA was measured with the NanoDrop spectrophotometer (ND2000, Thermo Scientific, DE, USA). Amplification of the V5-V7 regions of the 16S rRNA gene was performed using the primers 799F and 1193R (table S12). Sequencing libraries were generated using the NEXTFLEX Rapid DNA-Seq Kit (Bioo Scientific, USA) following the manufacturer's recommendations and sequenced on the Illumina MiSeq PE300 platform at the Majorbio Bio-Pharm Technology. Quality-filtered sequences were clustered into OTUs with a 97% sequence similarity using UPARSE (*63*). Representative sequences for each OTU were taxonomically classified with the RDP Classifier 2.13 (*64*) and annotated against the SILVA database (release 138). All OTUs identified as chloroplast and mitochondria were discarded from the data set.

Pseudomonas and _Acidovorax_ genomic analyses

To compare the metabolic potential of *Pseudomonas* and *Acidovorax* species, their representative genomes were collected by searching the NCBI's Genome Browser (https://www.ncbi.nlm.nih.gov/datasets/genome/) using "*Pseudomonas*" and "*Acidovorax*" as keywords, respectively. Genome selection was performed using standardized filtering criteria. For *Pseudomonas*, only reference genomes were included, while atypical genomes, MAGs, and genomes from large multi-isolate projects were excluded. Using these criteria, 359 *Pseudomonas* genomes were retained from the over 45,000 available genomes (accession date: October, 2024). For *Acidovorax*, only 12 reference genomes are available in NCBI. Therefore, we applied the same exclusion criteria (i.e., removal of atypical genomes, MAGs, and genomes from large multi-isolate projects) but did not restrict the dataset to reference genomes

only, resulting in a total of 128 *Acidovorax* genomes (accession date: October, 2024). Phylogenetic tree of the 359 *Pseudomonas* and 128 *Acidovorax* genomes were constructed using PhyloPhlAn 3.0 (*61*) based on concatenated alignments of up to 400 ubiquitously conserved proteins, and then visualized using iTOL (*62*). The habitat and location for *Pseudomonas* and *Acidovorax* species were sourced from the metadata of genomes downloaded from NCBI or manually extracted from publications. Instances where information remained unclear were labeled as "unknown".

BGCs in each genome were identified using antiSMASH v6.1.1(*65*) with the following parameters: --genefinding-tool prodigal --tigrfam --cc-mibig --rre --cb-general --cb-knownclusters --cb-subclusters --asf --pfam2go --smcog-trees. Each BGC was functionally characterized based on the predicted product types defined in BiG-SCAPE v1.1.5 (*66*).

NaCl tolerance of *Pseudomonas* and *Acidovorax* type strains

NaCl tolerance data for type strains of *Pseudomonas* and *Acidovorax* were compiled through a systematic survey of published literatures (accessed 1 February 2026), using the List of Prokaryotic names with Standing in Nomenclature (LPSN; https://lpsn.dsmz.de) as the reference database. In total, NaCl tolerance information was available for 321 of 362 *Pseudomonas* and 14 of 22 *Acidovorax* type strains (table S6).

AntiSAMSH prediction and construction of NAGGN synthetic gene mutants in *Pseudomonas* strains

Based on the genome sequences of *Pseudomonas* strains XN05-1 and YE17, the secondary metabolic gene cluster was predicted using the antiSMASH 7.1.0 online website (https://antismash.secondarymetabolites.org/). Three genes (ctg1_1282 to ctg1_1284 in strain XN05-1 and ctg1_3641 to ctg1_3643 in strain YE17, named *nbsABC*) are implicated in the biosynthesis of NAGGN (table S9). Mutants of *nbsABC* were generated via tri-parental conjugation using the suicide vector pK18mob*sacB* (*19*).

Specifically, the upstream and downstream fragments of genomic DNA from strains XN05-1 were amplified using the primers XN05-1-NAGGN-UF/UR and XN05-1-NAGGN-DF/DR, respectively. The amplified fragments were purified and cloned into the suicide vector pK18mob*sacB*. The resulting recombinant plasmid was then transformed into an Amp^R-derivative of XN05-1, with the aid of the helper plasmid pRK2013. Potential mutants were grown on NA medium containing 15% (w/v) sucrose to facilitate the excision of the suicide vector from the chromosome. The final mutant was confirmed using primers XN05-1-NAGGN-UF/XN05-1-NAGGN-DR and designated Δ*nbsABC*$_{\text{XN05-1}}$. The NAGGN biosynthesis gene mutant of YE17, named Δ*nbsABC*$_{\text{YE17}}$, was constructed following the same procedure using the corresponding primers. The primers used are listed in table S12.

Salt tolerant of wild-type and NAGGN biosynthesis mutants of *Pseudomonas*

To evaluate the salt tolerance of wild-type and NAGGN biosynthesis mutants, growth kinetics of each strain were monitored across a range of NaCl concentrations (0-8%, w/v) in nutrient broth (NB) media (10 g/L peptone, 3 g/L beef extract, pH 7.2 ± 0.2). In a 96-well microplate, 198 μL of medium containing different NaCl concentrations was added to each well, followed by 2 μL of bacterial suspension (OD_{600} = 0.4). Each treatment was performed in triplicate. Microplates were incubated at 28°C with shaking at 180 rpm to ensure adequate aeration and prevent cell precipitation. The OD_{600} values were measured every 4 h over a 36-h period to capture the full growth profile.

Root colonization analysis

To investigate the colonization of strains XN05-1 and YE17 on soybean roots under control and salt stress conditions, the strains were labeled with GFP. The GFP-expressing plasmid *pBBR1MCS5-Tac-EGFP* was transformed into the recipient bacterial cells via triparental conjugation, with pRK2013 used as the helper strain. GFP-labeled strains were cultured on nutrient agar (NA) plates supplemented with gentamicin (final concentration, 30 μg/mL). A single colony was then transferred into

NB medium without antibiotic and cultured overnight. The culture was harvested by centrifugation, and resuspended in sterile water to an optical density of OD_{600} = 1.0. Subsequently, 1 mL of the prepared suspension was added to 39 mL of 1/8-strength Hoagland solution (either without NaCl or supplemented with 50 mM NaCl) for co-cultivation with soybean (cv. Zhonghuang 13) seedlings (*67, 68*). Each treatment was conducted in triplicate. After three days of inoculation, the roots of the soybean seedlings were rinsed under running tap water and observed using a confocal microscope (Leica Microsystems, Wetzlar, Germany). Fluorescence images were quantitatively analyzed using Image J software v1.54g. Briefly, each image was divided into consecutive regions (15.0 × 1.0 pixels) along the root axis to cover the entire imaged root system. The integrated density of each selected region was then measured to quantify fluorescence intensity.

Motility and growth of GFP-labeled and wild-type strains

Bacterial motility was determined using a semi-solid agar assay (1% peptone, 0.5% NaCl, and 0.3% agar). Overnight cultures grown in NB medium at 28 ℃ with shaking were adjusted to an OD_{600} of 0.4. Then, 2 μL of each bacterial suspension was spotted onto the semi-solid agar plates and incubated at 28 ℃ for 18 h. The diameter of the spreading zone was measured as an indicator of bacterial motility. Each treatment included six biological replicates. Growth was assessed according to the method described above for wild-type and NAGGN biosynthesis mutants.

Greenhouse and field experiments with *Pseudomonas* inoculation

Pseudomonas strains XN05-1 and YE17 were inoculated onto soybean plants with or without salt stress under greenhouse condition. In brief, soybean seeds (cv. Zhonghuang 13) were surface-disinfected as described above. Five seeds were sown per pot containing 60 g of sterilized vermiculite, with ten replicate pots per treatment. *Pseudomonas* strains XN05-1 and YE17 were cultured overnight in NB medium, followed by centrifugation at 4°C and 4000 rpm to concentrate the bacterial cells. The

pellets were then resuspended in sterile water, and inoculated into 10-day-old soybean seedlings with 20 mL bacterial suspension (~2.6×10^7 CFU/mL) for each pot. *Pseudomonas* were applied three times at a two-day interval. After the final inoculation, salt stress was imposed by applying 300 mM NaCl (60 mL per pot, applied as 20 mL per day for three consecutive days). Control plants received 60 mL of sterile water applied in the same manner. All plants were incubated in a climate chamber as described above, and watered regularly with sterile water from the top. Watering was controlled to prevent drainage, and pots were placed on base trays to retain excess water and minimize bacterial loss. The growth phenotypes, root morphology, root Na^+ and K^+ contents, root lignin levels, and root RNA-seq were analyzed 10 days after the salt treatment. At the end of the experiment, *Pseudomonas* were quantified from soybean roots at a density of > 4.2×10^6 copies per gram of fresh root, confirming persistent root colonization. Quantification of *Pseudomonas* was performed as previously described by Zheng et al. (*19*).

A field experiment was conducted in natural saline soils (salinity of 0.42%) at Dongying, Shandong Province (37°17′28″N, 118°38′28″E), with treatments consisting of a non-inoculated control and two *Pseudomonas*-inoculated groups (strains XN05-1 and YE17). Each treatment was replicated three times in plots measuring 5 m × 7 m, arranged in a randomized block design. Soybean seeds (cv. Zhonghuang 13) were grown with an inter-row spacing of 40 cm and an intra-row spacing of 10 cm. Overnight cultures of *Pseudomonas* strains XN05-1 and YE17 were diluted by fourfold, and then used to coat soybean seeds at a dosage of 40 mL/kg. Control seeds received equal amounts of sterile water in the same manner. The treated seeds were sown in the designated plots. At 40 days after planting, each plot was treated with 100 L of a 50-fold diluted *Pseudomonas* suspension (prepared from an overnight culture) via root irrigation. Soybean plants were harvested at 70 days after planting to determine root weight, nodule number and pod number.

Root morphology observation

Soybean roots were gently rinsed with water, spread evenly on a transparent tray, and scanned using root scanner (Epson V700, Beijing, China). Root morphological parameters, including length, surface area, and volume, were analyzed using WinRHIZO Pro v2007 (Regent Instruments, Canada).

Determination of root Na^+ and K^+ contents

The root samples were dried at 65°C until a constant weight was achieved, and the final dry mass was recorded. Subsequently, the samples were digested in nitric acid at 110°C for a duration of 6 hours. The concentrations of Na^+ and K^+ were quantified using inductively coupled plasma optical emission spectrometry (ICP-OES; Varian, Inc., USA).

Soybean root RNA-seq analysis

Root samples of soybean grown in vermiculite with or without salt stress (300 mM NaCl) were collected for RNA extraction and sequencing. Total RNA was extracted using TRIzol® Reagent according to the manufacturer's instructions. RNA sequencing libraries were prepared using a poly(A) selection strategy to enrich mRNA and sequenced on the NovaSeq 6000 platform. The raw paired end reads were trimmed and quality controlled by fastp (*69*) with default parameters. Quality-filtered reads were mapped exclusively to a reference soybean genome (Glycine_max_v2.1; http://plants.ensembl.org/Glycine_max/Info/Index) using HISAT2 v2.2.1 (*70*). Normalized read counts were calculated using the transcripts per kilobase million (TPM) method. DEGs were identified using DESeq2 v1.24.0 (*71*). Genes with an absolute $|\log_2$ fold change$| > 2$ and a P-value < 0.05 were considered significantly differentially expressed. GO and KEGG pathway enrichment analyses of the DEGs were performed using the Goatools v0.6.5 (*72*) and Python SciPy v1.13.0 packages (*73*), respectively.

Quantification of lignin content in soybean roots

The soybean root samples were dried at 80°C until reaching a constant weight. Subsequently, the dried roots were finely ground and passed through a 40-mesh sieve. Lignin content in the soybean roots was extracted and quantified using a commercial kit purchased from Solarbio (Beijing, China). In brief, 3 mg of dried root sample was subjected to acetylation of the phenolic hydroxyl groups in lignin. The resulting supernatant was thoroughly mixed with glacial acetic acid, followed by measurement of absorbance at 280 nm. The lignin content was then calculated using the formula provided in the manual.

Vector construction for the generation of transgenic soybean plants

To construct the *GmCAD* overexpression vector, the *GmCAD* coding sequence was first amplified from soybean root cDNA using primers *GmCAD*-F and *GmCAD*-R. Primers *GmCAD*-pFGC5941-F and *GmCAD*-pFGC5941-R were used to introduce restriction sites. The cloning vector pFGC5941 was digested with *Bam*HI and *Sam*I, and the amplified *GmCAD* product with restriction sites was subsequently ligated into the pFGC5941 vector (*74*). The recombinant vector was transformed into *Escherichia coli* DH5α for propagation. Plasmid DNA from positive clones was then transformed into *Agrobacterium rhizogenes* K599. Transformants were selected on kanamycin-containing medium (50 μg/mL) and sequenced for validation. The overexpression vectors of *Gm4CL* and *GmCOMT* were constructed following the same procedure using the corresponding primers. All primer sequences are provided in table S12.

To generate *Gmcad* loss-of-function mutants, CRISPR/Cas9-mediated genome editing was performed following previous study (*75*). Target fragments were cloned into the pHSE401 vector via Golden Gate assembly using BsaI, and the resulting constructs were introduced into *A. rhizogenes* K599 for soybean transformation. Mutant lines of *Gm4cl* and *Gmcomt* were constructed in parallel using the same cloning and transformation workflow. Primer sequences used for cloning are provided in table S12.

Soybean hairy-root transformation and phenotypic analysis

To generate composite soybean plants, *A. rhizogenes* strain K599 harboring overexpression vector was used to infect soybean seedlings following a previously described protocol with minor modifications (*76*). Briefly, seeds of the soybean cultivar Zhonghuang 13 were germinated for 4 days before inoculation with *A. rhizogenes* K599. Once transgenic hairy roots reached a length of 3-5 cm, the primary root was excised, and the plants were transferred to 1/8-strength Hoagland solution for 7 days. Initial hairy root lengths were recorded prior to salt treatment, after which the plants were transferred to fresh 1/8-Hoagland solution containing either 0 mM or 50 mM NaCl. After two weeks of salt stress, root lengths were measured again, and relative elongation was calculated as: (root length after salt treatment – root length before salt treatment)/ root length before salt treatment. Roots were then harvested for subsequent gene expression analysis. The expression levels of *GmCAD*, *Gm4CL*, and *GmCOMT* were validated by qRT-PCR with specific primers (table S12).

For the *Pseudomonas* inoculation experiment, *A. rhizogenes* strain K599 carrying the CRISPR/Cas9 vector was used to infect soybean seedlings. Transgenic soybean hairy roots (20 days post-infection) were inoculated with a mixture of *Pseudomonas* strains XN05-1 and YE17. Co-inoculation was chosen because the two isolates exhibited highly similar functional traits, including root colonization, intrinsic salt tolerance, mitigation of soybean salt stress, and induction of comparable root transcriptomic responses, and therefore was unlikely to confound validation of the lignin-disruption experiment. Moreover, co-inoculation may better reflect ecologically relevant conditions, as these strains naturally coexist in microbial communities. All plants were subsequently treated with 50 mM NaCl in a hydroponic system containing Hoagland solution. After 15 days of NaCl treatment, the salt injury index was calculated according to previous study (*77*).

Statistical analyses

Principal coordinate analysis (PCoA) was used to ordinate the bacterial community based on the Bray-Curtis distance using the vegan v2.7.1 and ggplot2 v3.5.2 packages in R v3.5.3. PERMANOVA was calculated based on Bray-Curtis distance with 999 permutations in R. Heatmap of the top 10 bacterial genera of control and salt treatment for acidic and alkaline soils was plotted using TBtools (*78*). Linear discriminant analysis (LDA) of effect size (LEfSe) was applied to identify the enriched bacterial taxa in control and salt treatments for all plant species. All statistical analyses were performed using two-sided *t*-tests, unless otherwise specified.

References

1. M. Zhou, K. Butterbach-Bahl, H. Vereecken, N. Brüggemann, A meta-analysis of soil salinization effects on nitrogen pools, cycles and fluxes in coastal ecosystems. *Global Change Biol.* **23**, 1338-1352 (2017).
2. G. Zhang, J. Bai, Y. Zhai, J. Jia, Q. Zhao, W. Wang, X. Hu, Microbial diversity and functions in saline soils: A review from a biogeochemical perspective. *J. Adv. Res.* **59**, 129-140 (2023).
3. J. Rozema, T. Flowers, Crops for a salinized world. *Science* **322**, 1478-1480 (2008).
4. A. Hassani, A. Azapagic, N. Shokri, Global predictions of primary soil salinization under changing climate in the 21st century. *Nat. Commun.* **12**, 6663 (2021).
5. X. Tang, X. Mu, H. Shao, H. Wang, M. Brestic, Global plant-responding mechanisms to salt stress: physiological and molecular levels and implications in biotechnology. *Crit. Rev. Biotechnol.* **35**, 425-437 (2015).
6. H. Zhou, H. Shi, Y. Yang, X. Feng, X. Chen, F. Xiao, H. Lin, Y. Guo, Insights into plant salt stress signaling and tolerance. *J. Genet. Genomics* **51**, 16-34 (2024).
7. Y. Qin, I. S. Druzhinina, X. Pan, Z. Yuan, Microbially mediated plant salt tolerance and microbiome-based solutions for saline agriculture. *Biotechnol. Adv.* **34**, 1245-1259 (2016).
8. H. Etesami, G. A. Beattie, Mining halophytes for plant growth-promoting halotolerant bacteria to enhance the salinity tolerance of non-halophytic crops.

774 *Front. Microbiol.* **9**, 00148 (2018).
775 9. Z. Wang, Y. Song, Toward understanding the genetic bases underlying plant-
776 mediated “cry for help” to the microbiota. *iMeta* **1**, (2022).
777 10. S. A. Rolfe, J. Griffiths, J. Ton, Crying out for help with root exudates: adaptive
778 mechanisms by which stressed plants assemble health-promoting soil
779 microbiomes. *Curr. Opin. Microbiol.* **49**, 73-82 (2019).
780 11. Y. Xu, Z. Wang, J. Wu, Y. Yue, Y. Ren, Y. Pan, J. Li, C. Liu, R. Borriss, X. Liu, J.
781 Qiao, Y.-W. Lee, H. Wu, F. Dini-Andreote, Q. Shen, W. Xiong, X. Gao, R. L.
782 Berendsen, Q. Gu, Keystone *Pseudomonas* species in the wheat phyllosphere
783 microbiome mitigate Fusarium head blight by altering host pH. *Cell Host Microbe*
784 **33**, 2052-2066.e2054 (2025).
785 12. I. A. Stringlis, K. Yu, K. Feussner, R. de Jonge, S. Van Bentum, M. C. Van Verk,
786 R. L. Berendsen, P. A. H. M. Bakker, I. Feussner, C. M. J. Pieterse, MYB72-
787 dependent coumarin exudation shapes root microbiome assembly to promote plant
788 health. *Proc. Natl. Acad. Sci. U.S.A* **115**, E5213-E5222 (2018).
789 13. P. Yu, X. He, M. Baer, S. Beirinckx, T. Tian, Y. A. T. Moya, X. Zhang, M.
790 Deichmann, F. P. Frey, V. Bresgen, C. Li, B. S. Razavi, G. Schaaf, N. von Wirén,
791 Z. Su, M. Bucher, K. Tsuda, S. Goormachtig, X. Chen, F. Hochholdinger, Plant
792 flavones enrich rhizosphere Oxalobacteraceae to improve maize performance
793 under nitrogen deprivation. *Nat. Plants* **7**, 481-499 (2021).
794 14. X. He, D. Wang, Y. Jiang, M. Li, M. Delgado-Baquerizo, C. McLaughlin, C.
795 Marcon, L. Guo, M. Baer, Y. A. T. Moya, N. von Wirén, M. Deichmann, G. Schaaf,
796 H.-P. Piepho, Z. Yang, J. Yang, B. Yim, K. Smalla, S. Goormachtig, F. T. de Vries,
797 H. Hüging, M. Baer, R. J. H. Sawers, J. C. Reif, F. Hochholdinger, X. Chen, P. Yu,
798 Heritable microbiome variation is correlated with source environment in locally
799 adapted maize varieties. *Nat. Plants* **10**, 598-617 (2024).
800 15. Q. Huang, R. Wang, Q. Ding, F. Liao, L. Zhu, M. Huang, J. Li, J. Zeng, Q. Shen,
801 M. Wang, S. Guo, Low-nitrogen input enriches *Massilia* bacteria in the
802 phyllosphere to improve blast resistance in rice. *New Phytol.* **248**, 3151-3167

(2025).

16. H. Liu, J. Li, B. K. Singh, Harnessing co-evolutionary interactions between plants and *Streptomyces* to combat drought stress. *Nat. Plants* **10**, 1159-1171 (2024).
17. D. Naylor, S. Degraaf, E. Purdom, D. Coleman-Derr, Drought and host selection influence bacterial community dynamics in the grass root microbiome. *ISME J.* **11**, 2691-2704 (2017).
18. C. Santos-Medellín, Z. Liechty, J. Edwards, B. Nguyen, B. Huang, B. C. Weimer, V. Sundaresan, Prolonged drought imparts lasting compositional changes to the rice root microbiome. *Nat. Plants* **7**, 1065-1077 (2021).
19. Y. Zheng, X. Cao, Y. Zhou, S. Ma, Y. Wang, Z. Li, D. Zhao, Y. Yang, H. Zhang, C. Meng, Z. Xie, X. Sui, K. Xu, Y. Li, C.-S. Zhang, Purines enrich root-associated *Pseudomonas* and improve wild soybean growth under salt stress. *Nat. Commun.* **15**, 3520 (2024).
20. F. Wu, Z. Chen, X. Xu, X. Xue, Y. Zhang, N. Sui, Halotolerant *Bacillus* sp. strain RA coordinates *myo*-inositol metabolism to confer salt tolerance to tomato. *J. Integr. Plant Biol.* **66**, 1871-1885 (2024).
21. Y. Wang, Y. Yang, D. Zhao, Z. Li, X. Sui, H. Zhang, J. Liu, Y. Li, C.-S. Zhang, Y. Zheng, *Ensifer* sp. GMS14 enhances soybean salt tolerance for potential application in saline soil reclamation. *J. Environ. Manage.* **349**, 119488 (2024).
22. L. Feng, Q. Li, D. Zhou, M. Jia, Z. Liu, Z. Hou, Q. Ren, S. Ji, S. Sang, S. Lu, J. Yu, *B. subtilis* CNBG-PGPR-1 induces methionine to regulate ethylene pathway and ROS scavenging for improving salt tolerance of tomato. *Plant J.* **117**, 193-211 (2024).
23. N. Mehmood, M. Saeed, S. Zafarullah, S. Hyder, Z. F. Rizvi, A. S. Gondal, N. Jamil, R. Iqbal, B. Ali, S. Ercisli, M. Kupe, Multifaceted impacts of plant-beneficial *Pseudomonas* spp. in managing various plant diseases and crop yield improvement. *ACS Omega* **8**, 22296-22315 (2023).
24. S. Sah, S. Krishnani, R. Singh, *Pseudomonas* mediated nutritional and growth promotional activities for sustainable food security. *Curr. Res. Microb. Sci.* **2**,

100084 (2021).

25. R. Yang, Q. Shi, T. Huang, Y. Yan, S. Li, Y. Fang, Y. Li, L. Liu, L. Liu, X. Wang, Y. Peng, J. Fan, L. Zou, S. Lin, G. Chen, The natural pyrazolotriazine pseudoiodinine from *Pseudomonas mosselii* 923 inhibits plant bacterial and fungal pathogens. *Nat. Commun.* **14**, 734 (2023).
26. A. Meliani, A. Bensoltane, L. Benidire, K. Oufdou, Plant growth-promotion and IAA secretion with *Pseudomonas fluorescens* and *Pseudomonas putida*. *Res. Rev. J. Bot. Sci.* **6**, 16-24 (2017).
27. V. Vives-Peris, A. Gómez-Cadenas, R. M. Pérez-Clemente, Salt stress alleviation in citrus plants by plant growth-promoting rhizobacteria *Pseudomonas putida* and *Novosphingobium* sp. *Plant Cell Rep.* **37**, 1557-1569 (2018).
28. S. Samaddar, P. Chatterjee, A. Roy Choudhury, S. Ahmed, T. Sa, Interactions between *Pseudomonas* spp. and their role in improving the red pepper plant growth under salinity stress. *Microbiol. Res.* **219**, 66-73 (2019).
29. M. Rajkumar, L. B. Bruno, J. R. Banu, Alleviation of environmental stress in plants: The role of beneficial *Pseudomonas* spp. *Crit. Rev. Environ. Sci. Technol.* **47**, 372-407 (2017).
30. T. R. Turner, E. K. James, P. S. Poole, The plant microbiome. *Genome Biol.* **14**, 209 (2013).
31. S. Compant, A. Samad, H. Faist, A. Sessitsch, A review on the plant microbiome: Ecology, functions, and emerging trends in microbial application. *J. Adv. Res.* **19**, 29-37 (2019).
32. G. Berg, D. Rybakova, M. Grube, M. Köberl, The plant microbiome explored: implications for experimental botany. *J. Exp. Bot.* **67**, 995-1002 (2016).
33. L. Xu, D. Naylor, Z. Dong, T. Simmons, G. Pierroz, K. K. Hixson, Y.-M. Kim, E. M. Zink, K. M. Engbrecht, Y. Wang, C. Gao, S. DeGraaf, M. A. Madera, J. A. Sievert, J. Hollingsworth, D. Birdseye, H. V. Scheller, R. Hutmacher, J. Dahlberg, C. Jansson, J. W. Taylor, P. G. Lemaux, D. Coleman-Derr, Drought delays development of the sorghum root microbiome and enriches for monoderm bacteria.

Proc. Natl. Acad. Sci. U.S.A **115**, E4284-E4293 (2018).

34. H. Liu, L. E. Brettell, Z. Qiu, B. K. Singh, Microbiome-mediated stress resistance in plants. *Trends Plant Sci.* **25**, 733-743 (2020).
35. S. Shi, A. E. Richardson, M. O'Callaghan, K. M. DeAngelis, E. E. Jones, A. Stewart, M. K. Firestone, L. M. Condron, Effects of selected root exudate components on soil bacterial communities. *FEMS Microbiol. Ecol.* **77**, 600-610 (2011).
36. H. Li, S. La, X. Zhang, L. Gao, Y. Tian, Salt-induced recruitment of specific root-associated bacterial consortium capable of enhancing plant adaptability to salt stress. *ISME J.* **15**, 2865-2882 (2021).
37. D. Haas, C. Keel, Regulation of antibiotic production in root-colonizing *Pseudomonas* spp. and relevance for biological control of plant disease. *Annu. Rev. Phytopathol.* **41**, 117-153 (2003).
38. D. Garrido-Sanz, P. Vesga, C. M. Heiman, A. Altenried, C. Keel, J. Vacheron, Relation of pest insect-killing and soilborne pathogen-inhibition abilities to species diversification in environmental *Pseudomonas protegens*. *ISME J.* **17**, 1369-1381 (2023).
39. V. Sandhya, S. Z. Ali, M. Grover, G. Reddy, B. Venkateswarlu, Effect of plant growth promoting *Pseudomonas* spp. on compatible solutes, antioxidant status and plant growth of maize under drought stress. *Plant Growth Regul.* **62**, 21-30 (2010).
40. J. Wang, Y. Wang, S. Lu, H. Lou, X. Wang, W. Wang, AlgU mediates hyperosmotic tolerance in *Pseudomonas protegens* SN15-2 by regulating membrane stability, ROS scavenging, and osmolyte synthesis. *Appl. Environ. Microbiol.* **90**, e00596-00524 (2024).
41. M. Kurz, Y. Burch Adrien, B. Seip, E. Lindow Steven, H. Gross, Genome-driven investigation of compatible solute biosynthesis pathways of *Pseudomonas syringae* pv. syringae and their contribution to water stress tolerance. *Appl. Environ. Microbiol.* **76**, 5452-5462 (2010).
42. C. Freeman Brian, C. Chen, X. Yu, L. Nielsen, K. Peterson, A. Beattie Gwyn,

Physiological and transcriptional responses to osmotic stress of two *Pseudomonas syringae* strains that differ in epiphytic fitness and osmotolerance. *J. Bacteriol.* **195**, 4742-4752 (2013).

43. P. Mishra, J. Mishra, N. K. Arora, Plant growth promoting bacteria for combating salinity stress in plants – Recent developments and prospects: A review. *Microbiol. Res.* **252**, 126861 (2021).

44. H. Zhou, H. Shi, Y. Yang, X. Feng, X. Chen, F. Xiao, H. Lin, Y. Guo, Insights into plant salt stress signaling and tolerance. *J. Genet. Genomics* **51**, 16-34 (2024).

45. L. Colin, F. Ruhnow, J.-K. Zhu, C. Zhao, Y. Zhao, S. Persson, The cell biology of primary cell walls during salt stress. *Plant Cell* **35**, 201-217 (2023).

46. Y. Yu, D.-D. Guo, D.-H. Min, T. Cao, L. Ning, Q.-Y. Jiang, X.-J. Sun, H. Zhang, W.-s. Tang, S.-Q. Gao, Y.-B. Zhou, Z.-S. Xu, J. Chen, Y.-Z. Ma, M. Chen, X.-H. Zhang, Foxtail millet MYB-like transcription factor SiMYB16 confers salt tolerance in transgenic rice by regulating phenylpropane pathway. *Plant Physiol. Biochem.* **195**, 310-321 (2023).

47. J. Chang, Y. Guo, J. Yan, Z. Zhang, L. Yuan, C. Wei, Y. Zhang, J. Ma, J. Yang, X. Zhang, H. Li, The role of watermelon caffeic acid O-methyltransferase (*ClCOMT1*) in melatonin biosynthesis and abiotic stress tolerance. *Hortic. Res.* **8**, 210 (2021).

48. L. Yuan, J. Dang, J. Zhang, L. Wang, H. Zheng, G. Li, J. Li, F. Zhou, A. Khan, Z. Zhang, X. Hu, A glutathione S-transferase regulates lignin biosynthesis and enhances salt tolerance in tomato. *Plant Physiol.* **196**, 2989-3006 (2024).

49. G. V. Uritskiy, J. Diruggiero, J. Taylor, MetaWRAP—a flexible pipeline for genome-resolved metagenomic data analysis. *Microbiome* **6**, 1-13 (2018).

50. D. Li, R. Luo, C.-M. Liu, C.-M. Leung, H.-F. Ting, K. Sadakane, H. Yamashita, T.-W. Lam, MEGAHIT v1.0: A fast and scalable metagenome assembler driven by advanced methodologies and community practices. *Methods* **102**, 3-11 (2016).

51. D. D. Kang, F. Li, E. Kirton, A. Thomas, R. Egan, H. An, Z. Wang, MetaBAT 2: an adaptive binning algorithm for robust and efficient genome reconstruction from

metagenome assemblies. *PeerJ* **7**, e7359 (2019).

52. Y.-W. Wu, B. A. Simmons, S. W. Singer, MaxBin 2.0: an automated binning algorithm to recover genomes from multiple metagenomic datasets. *Bioinformatics* **32**, 605-607 (2016).
53. J. Alneberg, B. S. Bjarnason, I. De Bruijn, M. Schirmer, J. Quick, U. Z. Ijaz, L. Lahti, N. J. Loman, A. F. Andersson, C. Quince, Binning metagenomic contigs by coverage and composition. *Nat. Methods* **11**, 1144-1146 (2014).
54. M. R. Olm, C. T. Brown, B. Brooks, J. F. Banfield, dRep: a tool for fast and accurate genomic comparisons that enables improved genome recovery from metagenomes through de-replication. *ISME J.* **11**, 2864-2868 (2017).
55. D. H. Parks, M. Imelfort, C. T. Skennerton, P. Hugenholtz, G. W. Tyson, CheckM: assessing the quality of microbial genomes recovered from isolates, single cells, and metagenomes. *Genome Res.* **25**, 1043-1055 (2015).
56. P.-A. Chaumeil, A. J. Mussig, P. Hugenholtz, D. H. Parks, GTDB-Tk: a toolkit to classify genomes with the Genome Taxonomy Database. *Bioinformatics* **36**, 1925-1927 (2020).
57. D. H. Parks, M. Chuvochina, D. W. Waite, C. Rinke, A. Skarshewski, P.-A. Chaumeil, P. Hugenholtz, A standardized bacterial taxonomy based on genome phylogeny substantially revises the tree of life. *Nat. Biotechnol.* **36**, 996-1004 (2018).
58. D. Hyatt, G.-L. Chen, P. F. Locascio, M. L. Land, F. W. Larimer, L. J. Hauser, Prodigal: prokaryotic gene recognition and translation initiation site identification. *BMC Bioinf.* **11**, 119 (2010).
59. J. Huerta-Cepas, D. Szklarczyk, D. Heller, A. Hernández-Plaza, S. K. Forslund, H. Cook, D. R. Mende, I. Letunic, T. Rattei, Lars J. Jensen, C. von Mering, P. Bork, eggNOG 5.0: a hierarchical, functionally and phylogenetically annotated orthology resource based on 5090 organisms and 2502 viruses. *Nucleic Acids Res.* **47**, D309-D314 (2019).
60. J. Huerta-Cepas, K. Forslund, L. P. Coelho, D. Szklarczyk, L. J. Jensen, C. von

Mering, P. Bork, Fast genome-wide functional annotation through orthology assignment by eggNOG-mapper. *Mol. Biol. Evol.* **34**, 2115-2122 (2017).

61. F. Asnicar, A. M. Thomas, F. Beghini, C. Mengoni, S. Manara, P. Manghi, Q. Zhu, M. Bolzan, F. Cumbo, U. May, J. G. Sanders, M. Zolfo, E. Kopylova, E. Pasolli, R. Knight, S. Mirarab, C. Huttenhower, N. Segata, Precise phylogenetic analysis of microbial isolates and genomes from metagenomes using PhyloPhlAn 3.0. *Nat. Commun.* **11**, 2500 (2020).
62. I. Letunic, P. Bork, Interactive Tree Of Life (iTOL) v5: an online tool for phylogenetic tree display and annotation. *Nucleic Acids Res.* **49**, W293-W296 (2021).
63. R. C. Edgar, UPARSE: highly accurate OTU sequences from microbial amplicon reads. *Nat. Methods* **10**, 996-998 (2013).
64. Q. Wang, M. Garrity George, M. Tiedje James, R. Cole James, Naïve Bayesian classifier for rapid assignment of rRNA sequences into the new bacterial taxonomy. *Appl. Environ. Microbiol.* **73**, 5261-5267 (2007).
65. K. Blin, S. Shaw, A. M. Kloosterman, Z. Charlop-Powers, G. P. van Wezel, Marnix H. Medema, T. Weber, antiSMASH 6.0: improving cluster detection and comparison capabilities. *Nucleic Acids Res.* **49**, W29-W35 (2021).
66. J. C. Navarro-Muñoz, N. Selem-Mojica, M. W. Mullowney, S. A. Kautsar, J. H. Tryon, E. I. Parkinson, E. L. C. De Los Santos, M. Yeong, P. Cruz-Morales, S. Abubucker, A. Roeters, W. Lokhorst, A. Fernandez-Guerra, L. T. D. Cappelini, A. W. Goering, R. J. Thomson, W. W. Metcalf, N. L. Kelleher, F. Barona-Gomez, M. H. Medema, A computational framework to explore large-scale biosynthetic diversity. *Nat. Chem. Biol.* **16**, 60-68 (2020).
67. A. Elbeltagy, K. Nishioka, T. Sato, H. Suzuki, B. Ye, T. Hamada, T. Isawa, H. Mitsui, K. Minamisawa, Endophytic colonization and In planta nitrogen fixation by a *Herbaspirillum* sp. isolated from wild rice species. *Appl. Environ. Microbiol.* **67**, 5285-5293 (2001).
68. R. Liu, R. Li, Y. Li, M. Li, W. Ma, L. Zheng, C. Wang, K. Zhang, Y. Tong, G.

977 Huang, X. Li, X.-G. Zhu, C. You, Y. Zhong, H. Liao, Benzoic acid facilitates ANF
978 in monocot crops by recruiting nitrogen-fixing *Paraburkholderia*. *ISME J.* **18**,
979 wrae210 (2024).
980 69. S. Chen, Y. Zhou, Y. Chen, J. Gu, fastp: an ultra-fast all-in-one FASTQ
981 preprocessor. *Bioinformatics* **34**, i884-i890 (2018).
982 70. D. Kim, B. Langmead, S. L. Salzberg, HISAT: a fast spliced aligner with low
983 memory requirements. *Nat. Methods* **12**, 357-360 (2015).
984 71. M. I. Love, W. Huber, S. Anders, Moderated estimation of fold change and
985 dispersion for RNA-seq data with DESeq2. *Genome Biol.* **15**, 550 (2014).
986 72. D. V. Klopfenstein, L. Zhang, B. S. Pedersen, F. Ramírez, A. Warwick Vesztrocy,
987 A. Naldi, C. J. Mungall, J. M. Yunes, O. Botvinnik, M. Weigel, W. Dampier, C.
988 Dessimoz, P. Flick, H. Tang, GOATOOLS: A Python library for Gene Ontology
989 analyses. *Sci. Rep.* **8**, 10872 (2018).
990 73. P. Virtanen, R. Gommers, T. E. Oliphant, M. Haberland, T. Reddy, D. Cournapeau,
991 E. Burovski, P. Peterson, W. Weckesser, J. Bright, S. J. van der Walt, M. Brett, J.
992 Wilson, K. J. Millman, N. Mayorov, A. R. J. Nelson, E. Jones, R. Kern, E. Larson,
993 C. J. Carey, İ. Polat, Y. Feng, E. W. Moore, J. VanderPlas, D. Laxalde, J. Perktold,
994 R. Cimrman, I. Henriksen, E. A. Quintero, C. R. Harris, A. M. Archibald, A. H.
995 Ribeiro, F. Pedregosa, P. van Mulbregt, A. Vijaykumar, A. P. Bardelli, A. Rothberg,
996 A. Hilboll, A. Kloeckner, A. Scopatz, A. Lee, A. Rokem, C. N. Woods, C. Fulton,
997 C. Masson, C. Häggström, C. Fitzgerald, D. A. Nicholson, D. R. Hagen, D. V.
998 Pasechnik, E. Olivetti, E. Martin, E. Wieser, F. Silva, F. Lenders, F. Wilhelm, G.
999 Young, G. A. Price, G.-L. Ingold, G. E. Allen, G. R. Lee, H. Audren, I. Probst, J.
1000 P. Dietrich, J. Silterra, J. T. Webber, J. Slavič, J. Nothman, J. Buchner, J. Kulick,
1001 J. L. Schönberger, J. V. de Miranda Cardoso, J. Reimer, J. Harrington, J. L. C.
1002 Rodríguez, J. Nunez-Iglesias, J. Kuczynski, K. Tritz, M. Thoma, M. Newville, M.
1003 Kümmerer, M. Bolingbroke, M. Tartre, M. Pak, N. J. Smith, N. Nowaczyk, N.
1004 Shebanov, O. Pavlyk, P. A. Brodtkorb, P. Lee, R. T. McGibbon, R. Feldbauer, S.
1005 Lewis, S. Tygier, S. Sievert, S. Vigna, S. Peterson, S. More, T. Pudlik, T. Oshima,

T. J. Pingel, T. P. Robitaille, T. Spura, T. R. Jones, T. Cera, T. Leslie, T. Zito, T. Krauss, U. Upadhyay, Y. O. Halchenko, Y. Vázquez-Baeza, C. SciPy, SciPy 1.0: fundamental algorithms for scientific computing in Python. *Nat. Methods* **17**, 261-272 (2020).

74. Z. Guo, H. Cao, J. Zhao, S. Bai, W. Peng, J. Li, L. Sun, L. Chen, Z. Lin, C. Shi, Q. Yang, Y. Yang, X. Wang, J. Tian, Z. Chen, H. Liao, A natural uORF variant confers phosphorus acquisition diversity in soybean. *Nat. Commun.* **13**, 3796 (2022).
75. H.-L. Xing, L. Dong, Z.-P. Wang, H.-Y. Zhang, C.-Y. Han, B. Liu, X.-C. Wang, Q.-J. Chen, A CRISPR/Cas9 toolkit for multiplex genome editing in plants. *BMC Plant Biol.* **14**, 327 (2014).
76. C. Wang, X. Li, Y. Zhuang, W. Sun, H. Cao, R. Xu, F. Kong, D. Zhang, A novel miR160a–GmARF16–GmMYC2 module determines soybean salt tolerance and adaptation. *New Phytol.* **241**, 2176-2192 (2024).
77. A. R. Gurmani, S. U. Khan, A. Ali, T. Rubab, T. Schwinghamer, G. Jilani, A. Farid, J. Zhang, Salicylic acid and kinetin mediated stimulation of salt tolerance in cucumber (*Cucumis sativus* L.) genotypes varying in salinity tolerance. *Hortic. Environ. Biote.* **59**, 461-471 (2018).
78. C. Chen, H. Chen, Y. Zhang, H. R. Thomas, M. H. Frank, Y. He, R. Xia, TBtools: An integrative toolkit developed for interactive analyses of big biological data. *Mol. Plant* **13**, 1194-1202 (2020).

Acknowledgements

We thank Prof. Zhichang Chen (Fujian Agriculture and Forestry University) for kindly providing the pFGC5941 vector.

Funding

This work was supported by the National Natural Science Foundation of China (32570138 to Y.Z., 32402669 to Y.W., 32572904 to C.Z., 32171948 to C.M.), Youth Innovation Program of the Chinese Academy of Agricultural Sciences (Y2025QC35 to

Y.Z.), Shandong Province Natural Science Foundation (ZR2024JQ006 to J.L.), Young Talent of Lifting Engineering for Science and Technology in Shandong (SDAST2025QTA075 to Y.Z.), Agricultural Science and Technology Innovation Program of China (ASTIP-TRIC06 to Y.L., ASTIP No. CAAS-ZDRW202407 to Y.L., and ASTIP-TRIC-ZD04 to C.Z.) and Natural Environmental Research Council, UK (NE/S001352, NE/X000990 and NE/X014428 to J.D.T.).

Author contributions

Conceptualization: Y.Z., Y.W., Z.W., J.D.T., Y.L., J.L., D.Z., and C.Z. Methodology: Y.Z., Y.W., Z.W., Z.L., C.M., Q.R., and S.M. Validation: Y.Z., Y.W., Z.W. Z.L., J.L., D.Z., and C.Z. Formal analysis: Y.Z., Y.W., Z.W., and J.L. Investigation: Y.Z., Y.W., Z.W., Z.L., S.H., and X.S. Visualization: Y.Z., Y.W., Z.W., and Q.R. Funding acquisition: Y.Z., Y.W., C.Z., J.L., Y.L., C.M., and J.D.T. Supervision: Y.Z., C.Z., D.Z., J.L., and Y.L. Writing—original draft: Y.Z., Y.W., Z.W., J.D.T., and J.L. Writing—review and editing: Y.Z., Y.W., Z.W., Z.L., J.D.T., C.M., S.H., X.S., Q.R., S.M., Y.L., J.L., D.Z., and C.Z.

Competing interests

The authors declare they have no competing interests.

Data and materials availability

The raw reads of 16S rRNA gene barcoding data (BioProject: PRJCA028745; https://ngdc.cncb.ac.cn/gsa/search?searchTerm=PRJCA028745) and RNA-seq data from soybean roots (BioProject: PRJCA041248; https://ngdc.cncb.ac.cn/gsa/search?searchTerm=PRJCA041248) have been deposited in the Genome Sequence Archive of China National Center for Bioinformation. All data needed to evaluate the conclusions in the paper are present in the paper and/or the Supplementary Materials. The *nbsABC* mutant strains and GFP-labeled strains can be provided by Chinese Academy of Agricultural Sciences pending scientific review and

a completed material transfer agreement with C.Z. Requests for the *nbsABC* mutant strains and GFP-labeled strains should be submitted to: C.Z. at zhangchengsheng@caas.cn.

Figure legends

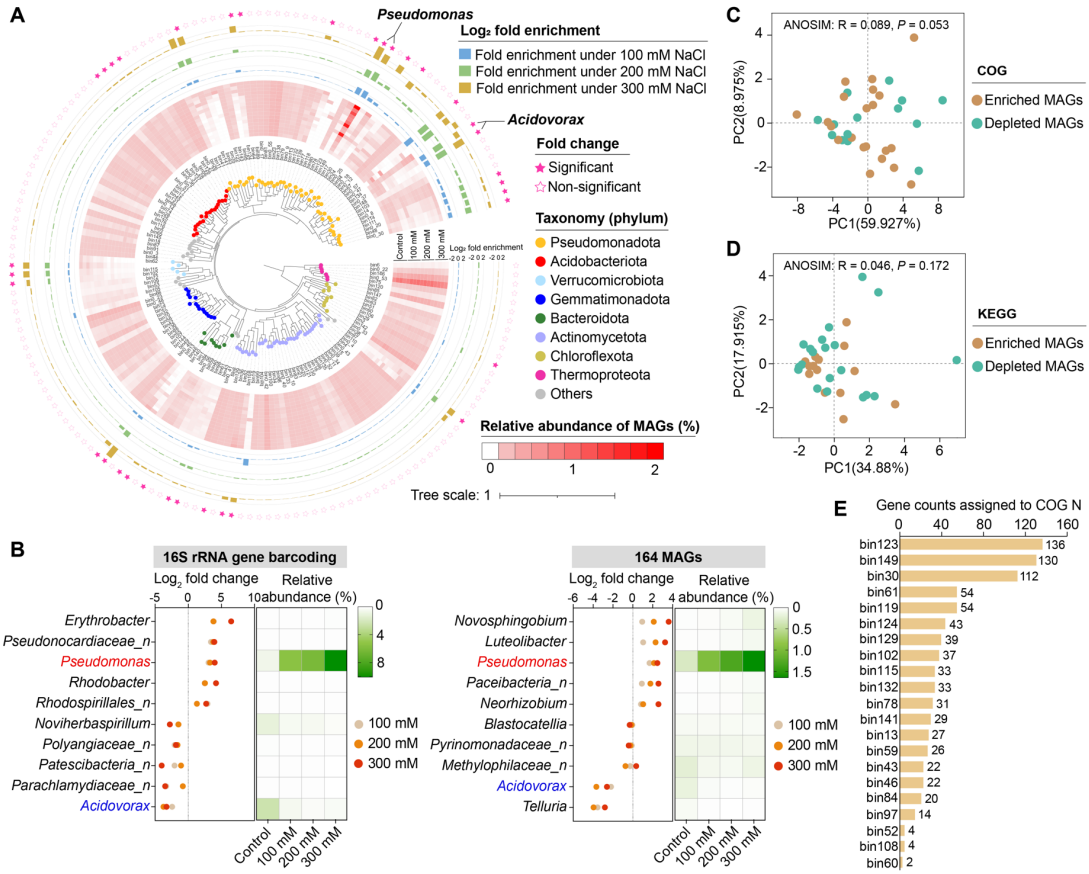

Fig. 1. Relative abundance and function of all metagenome-assembled genomes (MAGs) obtained in this study. (**A**) The maximum likelihood tree (IQ-TREE, based on concatenation of 400 ubiquitously conserved proteins) of the 164 MAGs was constructed using PhyloPhlAn 3.0. The tree scale indicates the number of substitutions per site. Tips of the tree are colored according to phylum-level taxonomy. The relative abundances of MAGs in different treatments (control, 100 mM, 200 mM and 300 mM NaCl) are shown in the heatmap, with four biological replicates for each treatment. Bar plots represent the fold enrichment under salt stress. The outer filled stars indicate MAGs exhibiting a significant change (two-sided Student's *t*-test, $P < 0.05$) between the control and at least one of the three salt treatment groups, whereas unfilled stars

denote non-significant differences. (**B**) The top 5 enriched or depleted genera in salt-treated rhizosphere soils of wild soybean based on 16S rRNA gene barcoding (*19*) and MAG datasets. Red and blue fonts indicate the consistent enriched or depleted taxon between 16S rRNA gene barcoding and MAG datasets, respectively. (**C** and **D**) The PCA ordination of COG (C) and KEGG (D) functions for the enriched and depleted MAGs. Statistical analysis was performed using ANOSIM (analysis of similarities). (**E**) Number of genes assigned to COG category N (cell motility) in salt-enriched MAGs.

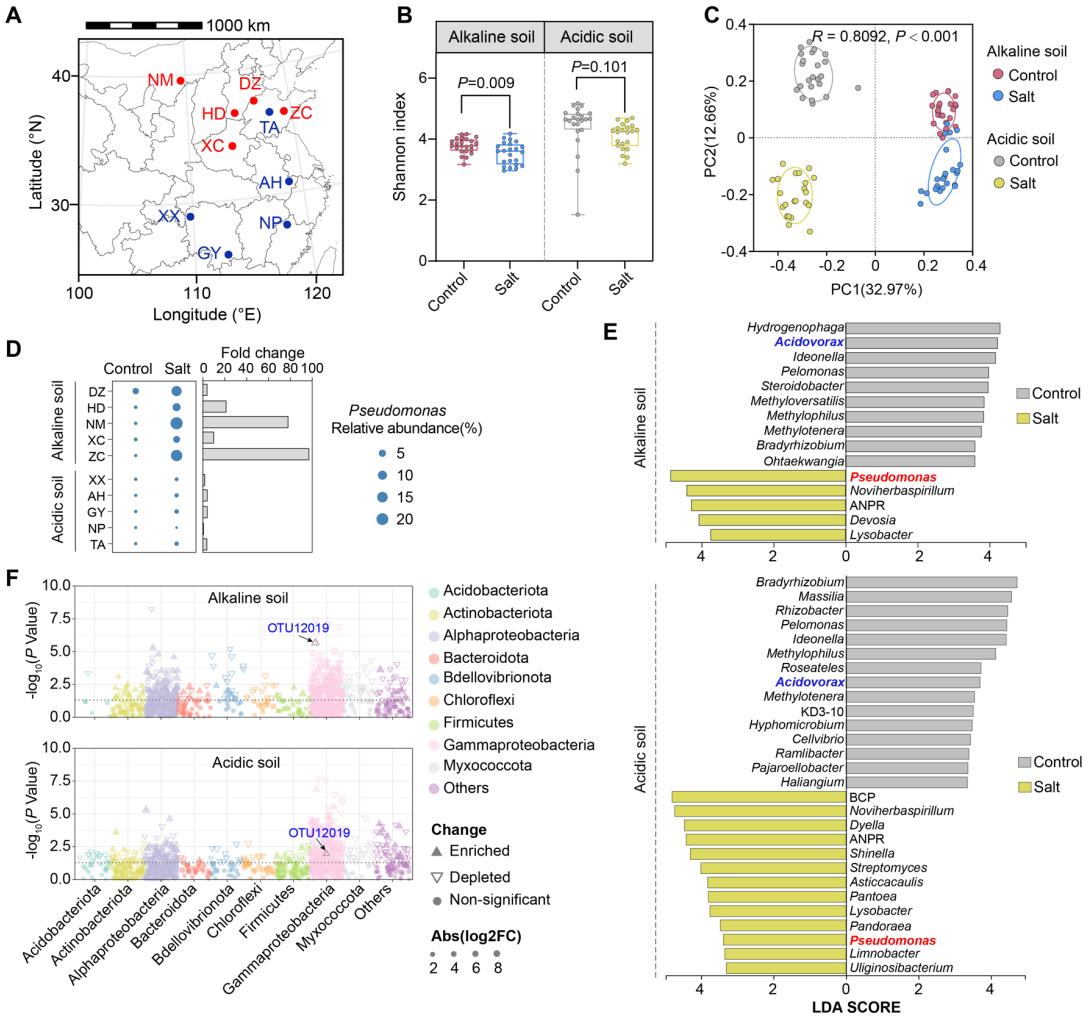

Fig. 2. The root-associated bacterial communities of wild soybean growing in alkaline and acidic soils. (**A**) The sampling sites of soil used for greenhouse experiment in this study. Word in red and blue colors indicate the sampling sites of alkaline soil and acidic soil, respectively. (**B**) Bacterial community alpha diversity (Shannon index) between control and salt stress for alkaline soil and acidic soil.

Statistical analyses were performed by two-sided Student's *t* test. Tops and bottoms of boxes represent 25th and 75th percentiles, respectively. Horizontal bars within boxes denote medians, and the upper and lower whiskers represent the range of non-outlier data values. (**C**) PCoA ordination of the Bray-Curtis dissimilarity matrix (OTU level) between control and salt stress for alkaline soil and acidic soil. Statistical analysis was performed using ANOSIM (analysis of similarities). (**D**) The relative abundance and fold change of *Pseudomonas* in the roots of wild soybean growing in alkaline and acidic soils. (**E**) The linear discriminant analysis (LDA) scores to identify the salt-enriched taxa at the genus level, determined by the LDA of effect size (LEfSe) analysis. Only taxa with LDA scores >3.5 in alkaline soil and >3.3 in acidic soil (to visualize *Pseudomonas*) are shown. Abbreviation: ANPR, *Allorhizobium-Neorhizobium-Pararhizobium-Rhizobium*; BCP, *Burkholderia-Caballeronia-Paraburkholderia*. (**F**) Manhattan plot displaying the taxonomic information of OTUs salt-enriched or depleted in the root of wild soybean growing in alkaline soil and acidic soil. The threshold of significant changed OTU is $P < 0.05$ & $|\log_2(\text{fold change})| > 1$. Salt stress in this experiment was applied with 300 mM NaCl. Statistical analyses were performed by two-sided Student's *t* test.

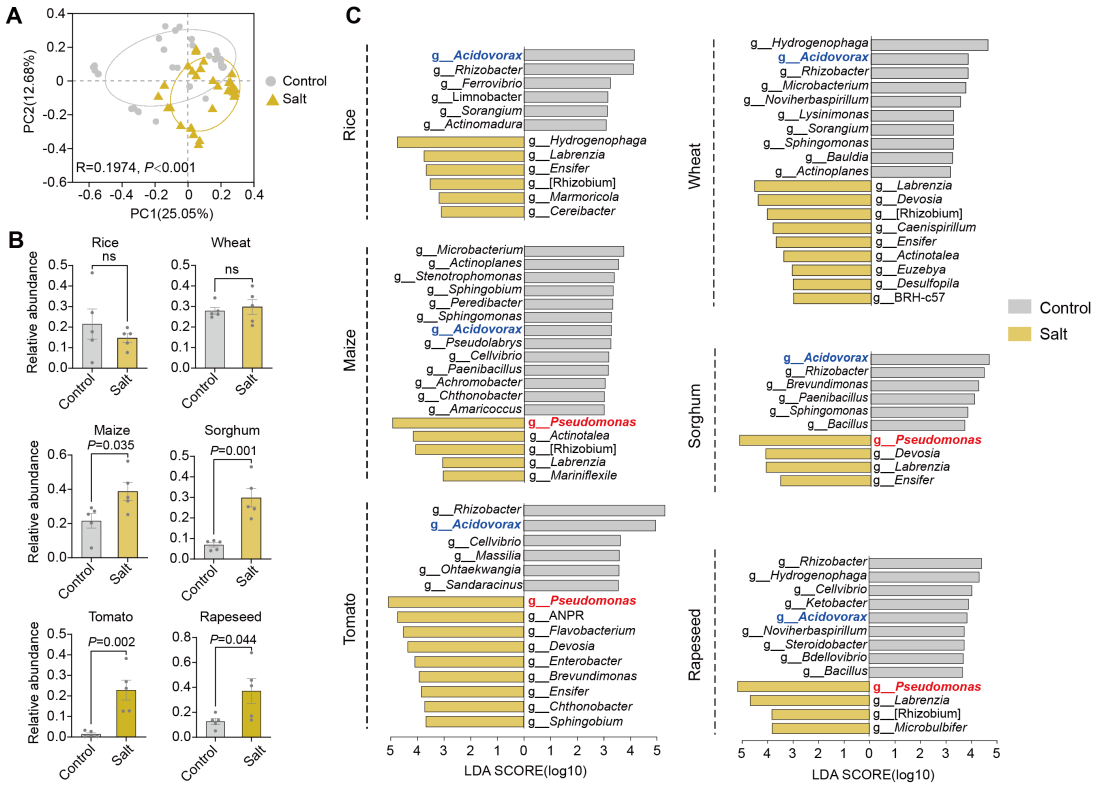

Fig. 3. The root-associated bacterial communities across different plant species. (**A**) PCoA ordination of the Bray-Curtis dissimilarity matrix (OTU level) between control and salt stress for all plants. Statistical analysis was performed using ANOSIM (analysis of similarities). (**B**) Relative abundance of *Pseudomonas* in the root-associated bacterial communities of control and salt stressed plants. Statistical analyses were performed by two-sided Student's *t* test. Values are means ± SEM ($n = 5$). (**C**) The LDA scores to identify the salt-enriched taxa at the genus (g) level, determined by the LEfSe analysis. Only taxa with the LDA score >3.5 are shown. Salt stress in this experiment was applied with 200 mM NaCl, as these crops have lower salt tolerance than wild soybean.

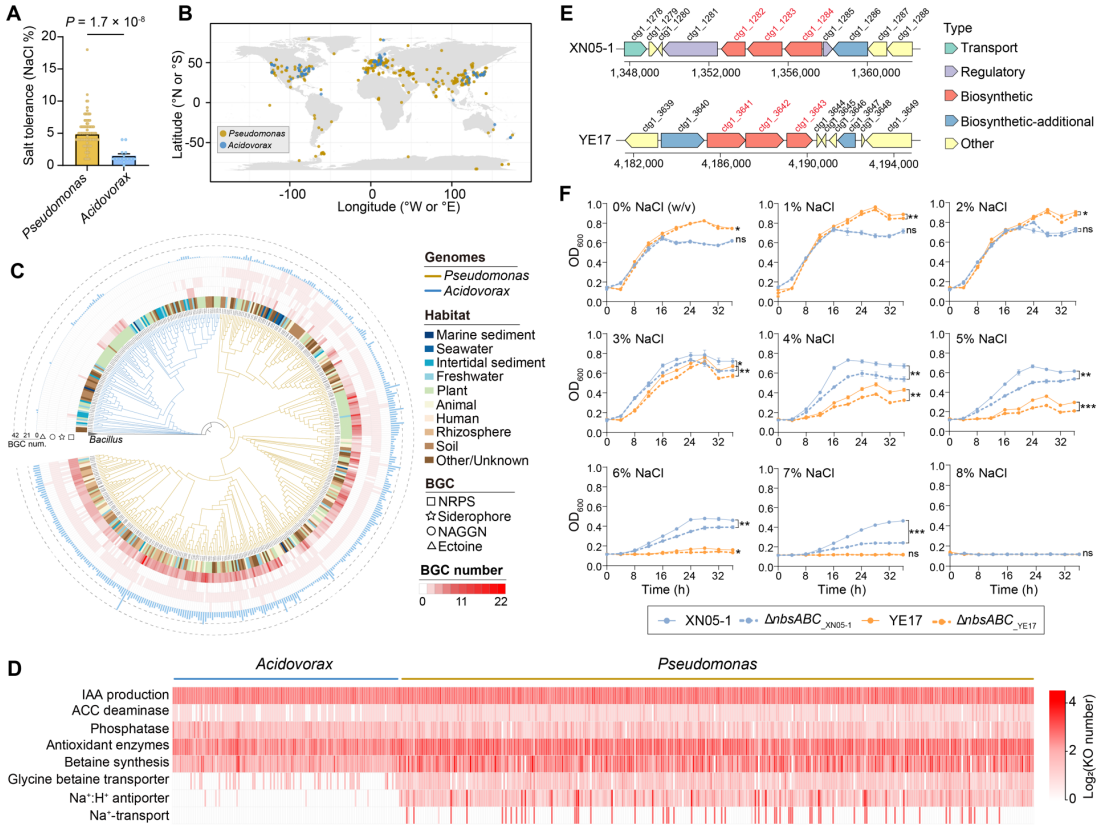

Fig. 4. The genetic potential of *Pseudomonas* for salt tolerance. (**A**) The salt tolerance of *Pseudomonas* (n = 78) and *Acidovorax* (n = 15) type strains reported in published literature (table S6). (**B**) The global distribution of *Pseudomonas* and *Acidovorax* species. The world map was generated using the maps and ggplot2 packages in R. (**C**) The maximum likelihood tree (IQ-TREE, based on concatenation of 400 ubiquitously conserved proteins) of *Pseudomonas* and *Acidovorax* genomes was constructed using PhyloPhlAn 3.0. The number of biosynthetic gene clusters (BGCs) related to salt tolerance are shown in the heatmap. Bar plots represent the total BGCs related to salt tolerance in each genome. (**D**) The predicted genes associated with plant growth-promoting traits and salt stress alleviation in *Pseudomonas* and *Acidovorax* genomes. Abbreviation: IAA, indole-3-acetic acid; ACC, 1-aminocyclopropane-1-carboxylate. (**E**) N-acetylglutaminylglutamine amide (NAGGN) biosynthetic gene cluster in genomes of *Pseudomonas* strains XN05-1 and YE17. Genes highlighted in red are those involved in the synthesis of NAGGN, which were subsequently knocked out in the following experiment. (**F**) The growth curves of wild-type and NAGGN

biosynthesis mutants (named *ΔnbsABC*) of *Pseudomonas* strains XN05-1 and YE17 across a range of NaCl concentrations (0-8%, w/v) over a 36-h period. Statistical analyses were performed using repeated-measures two-way analysis of variance (ANOVA) with the Geisser-Greenhouse correction. Values are means ± SEM (n = 3).

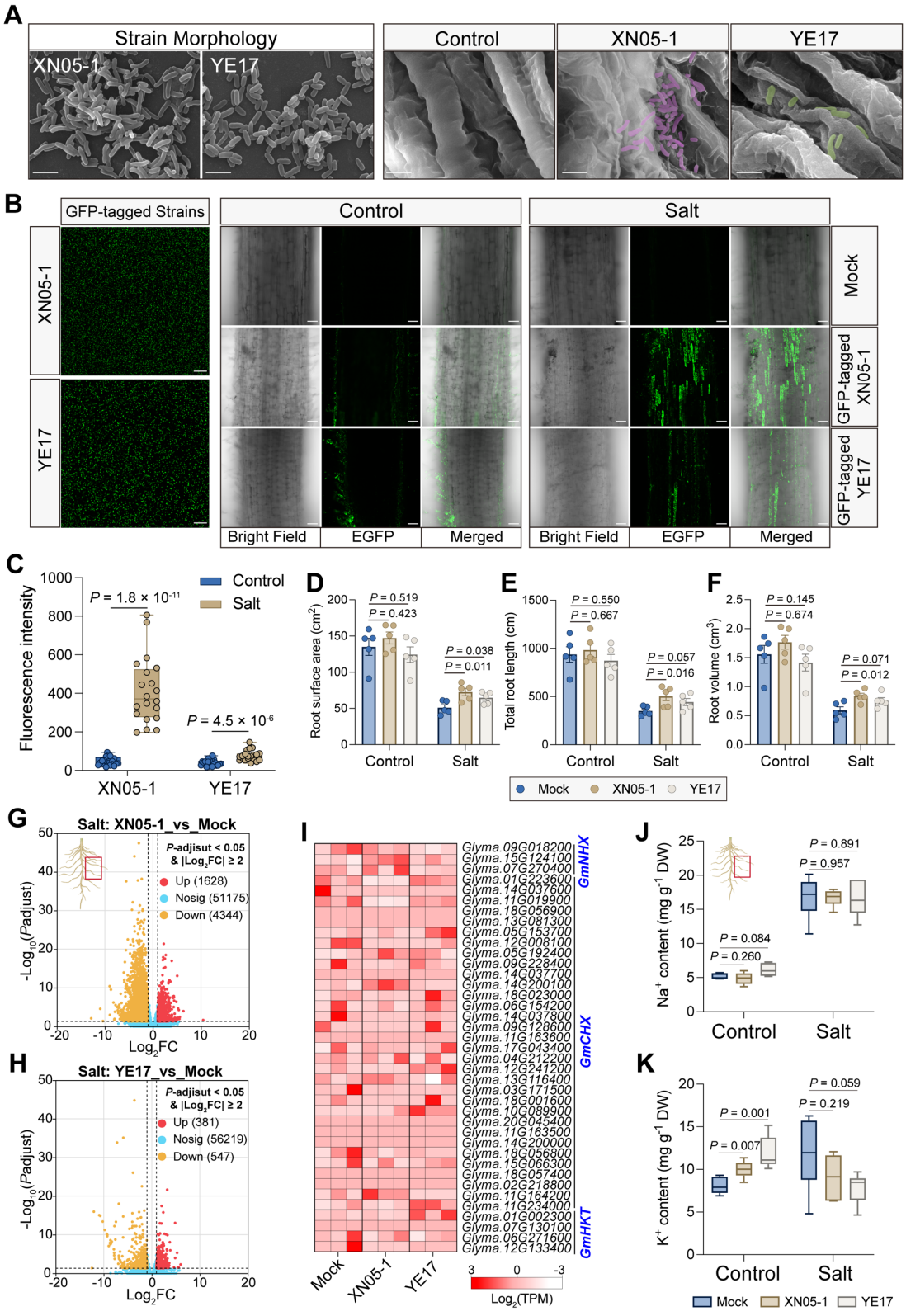

Fig. 5. Colonization by *Pseudomonas* XN05-1 and YE17 and the transcriptional response of soybean roots. (**A**) Scanning electron microscopy images of *Pseudomonas* strains alone or in the root surface. Bars = 2 μm. (**B**) Colonization patterns of strains

XN05-1 and YE17 in soybean roots visualized by GFP labeling. Bars = 75 μm. (**C**) Quantitative analysis of the fluorescent intensity, n = 20 image area (15.0 × 1.0 pixel). (**D** to **F**) Roots were characterized using the WinRHIZO root analysis system (n = 5), including total root length (D), root surface area (E), and root volume (F). (**G** and **H**) The volcano plots show the differentially expressed genes induced by inoculation with strains XN05-1 and YE17 under salt stress. (**I**) Expression levels of *GmNHX*, *GmCHX*, and *GmHKT* genes based on normalized TPM values. *GmNHX*: Na^+/H^+ Exchanger, Gm*CHX*: Cation/H^+ Exchanger, *GmHKT*: High-affinity K^+ Transporter. (**J** and **K**) Na^+ and K^+ content, n = 6 root samples. For figures A-C, *Pseudomonas* colonization experiment was conducted in Hoagland solution with or without salt stress (50 mM NaCl) to obtain clean roots for observation. For figures D-K, *Pseudomonas* inoculation experiment was performed in vermiculite with or without salt stress (300 mM NaCl). Exact P values were calculated using a two-tailed Student's t-test. All data are means ± SEM.

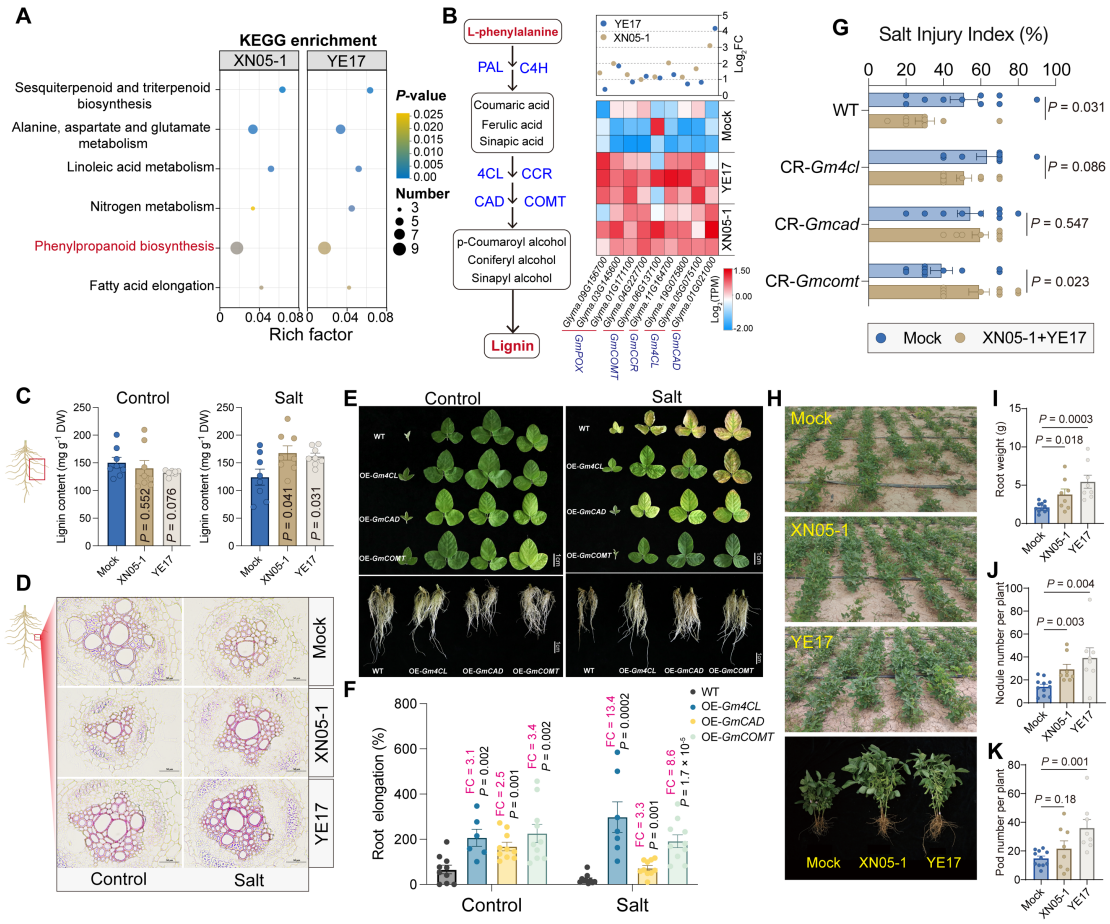

Fig. 6. *Pseudomonas* strains XN05-1 and YE17 regulate lignin biosynthesis in soybean. (**A**) KEGG enrichment analysis of differentially expressed genes in soybean root inoculated with XN05-1 and YE17 strains under salt stress (300 mM NaCl). (**B**) Expression level and fold change (FC) of lignin biosynthesis-related genes in soybean roots under mock inoculation and treatments with strains XN05-1 and YE17 under salt stress (300 mM NaCl). The gene heatmap was based on normalized TPM values. CAD: Cinnamyl alcohol dehydrogenase, 4CL: 4-Coumarate: CoA ligase, CCR: Cinnamoyl-CoA Reductase, COMT: Caffeic acid O-methyltransferase, POX: Peroxidase. (**C**) Lignin content in soybean roots under control and salt stress (300 mM NaCl) conditions following inoculation with XN05-1 and YE17 strains (n = 8). (**D**) Phloroglucinol was used for histochemical staining of root lignin, followed by sectioning and microscopic observation. Bars = 50 μm. (**E**) Phenotypes of transgenic plants under control and salt stress (50 mM NaCl) conditions in a hydroponic system. Bars = 1 cm. (**F**) Root elongation (%) of OE (overexpression) soybean lines (*OE-GmCAD*, *OE-Gm4CL*, and

OE-GmCOMT) under control and salt stress (50 mM NaCl) conditions (n = 6 or 10). Fold change (FC) = transgenic plants / WT (wild-type). (**G**) The salt injury index of WT and CR (CRISPR/Cas9 knockout) soybean lines (*CR-Gmcad*, *CR-Gm4cl*, and *CR-Gmcomt*) deficient in lignin biosynthesis after inoculating *Pseudomonas* (n = 8 to 10). (**H**) The soybean growth performance with or without *Pseudomonas* inoculation under field condition. (**I** to **K**) Root weight, nodule number and pod number of soybean with or without *Pseudomonas* inoculation under field condition (n = 8 or 11). Exact P values were calculated using a two-tailed Student's t-test. All data are means ± SEM.

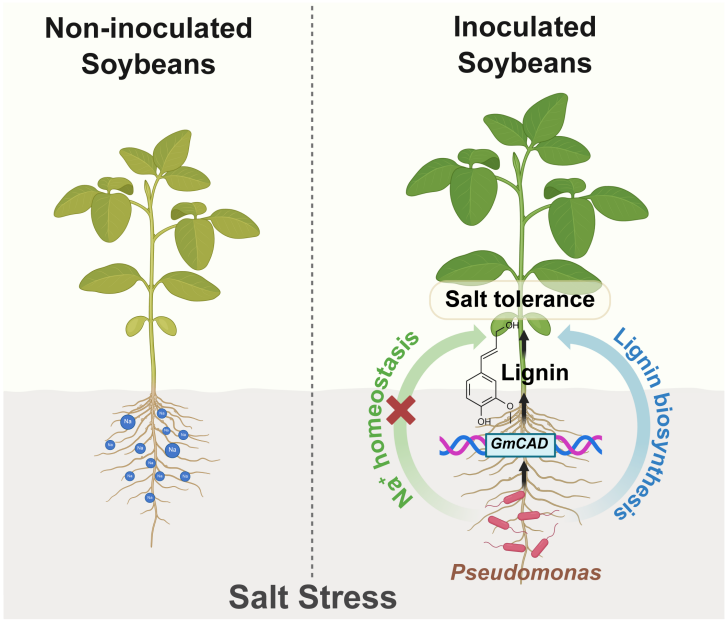

Fig. 7. Conceptual diagram of the conserved *Pseudomonas* in enhancing soybean salt tolerance. *Pseudomonas* functions as a specific signal that induces the expression of lignin biosynthesis-related genes, rather than Na^+ homeostasis, thereby promoting lignin deposition in the cell wall and improving plant salt tolerance. Created in BioRender. Zheng, Y. (2026) https://BioRender.com/5986dqo.

Supplementary Materials for

Pseudomonads associated to salt-stressed plants facilitate stress adaption of soybean through enhanced lignin biosynthesis

Yanfen Zheng *et al.*

Corresponding author: Cheng-Sheng Zhang, zhangchengsheng@caas.cn; Donglin Zhao, zhaodonglin@caas.cn; Jiwen Liu, liujiwen@ouc.edu.cn; Yiqiang Li, liyiqiang@caas.cn; Yanfen Zheng, zhengyanfen@caas.cn

The PDF file includes:

Figs. S1 to S13
Legends for tables S1 to S12

Other Supplementary Material for this manuscript includes the following:

Tables S1 to S12

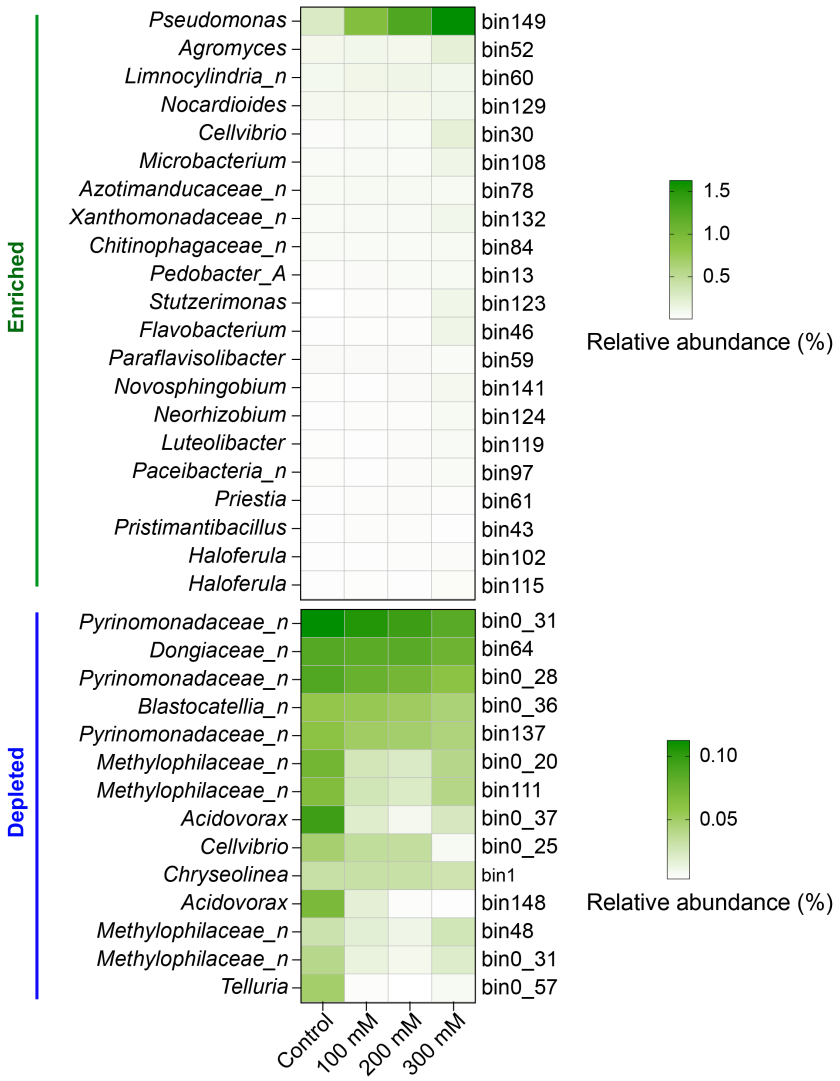

Fig. S1. The relative abundance of all enriched or depleted MAGs in rhizosphere soil of control and salt-treated wild soybean. Based on metagenomic data, 35 MAGs were detected with significant abundance changes between control and salt treatments, including 21 salt-enriched and 14 salt-depleted MAGs. Enriched or depleted MAGs were defined if their abundance differed significantly between the control and at least one of the three salt treatment groups (two-sided Student's *t*-test, $P < 0.05$). Values represent means from four biologically independent samples.

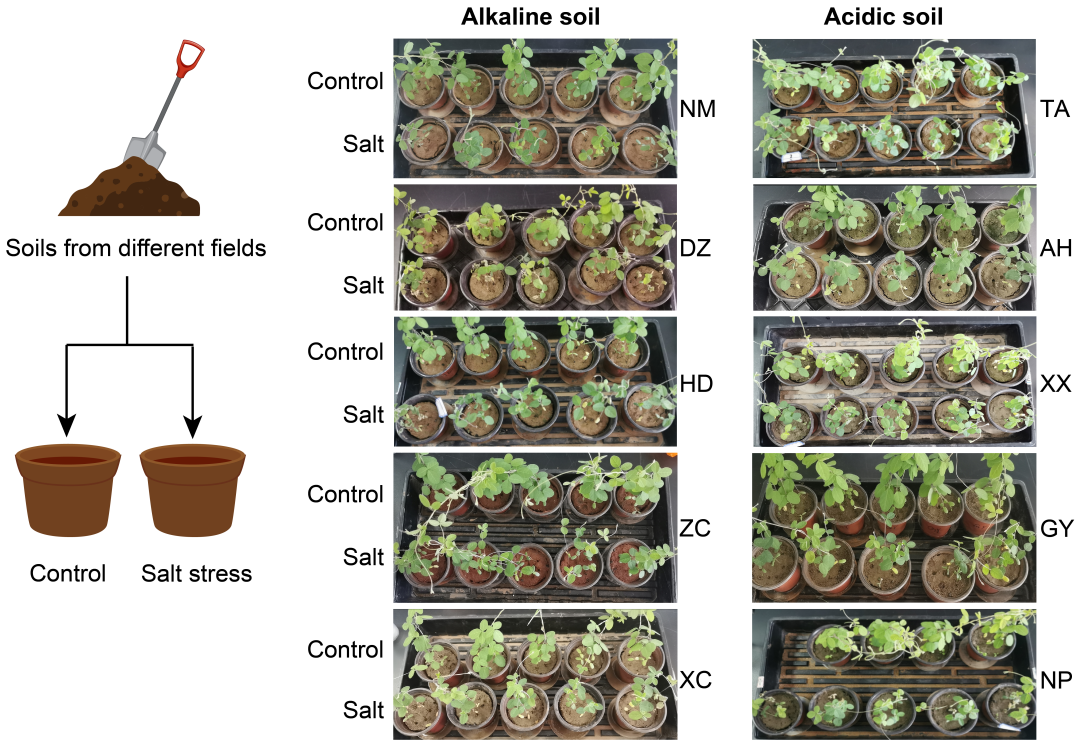

Fig. S2. Phenotype of wild soybean growing in alkaline and acidic soils under control and salt stress conditions. Bulk soils at a depth of 0-10 cm were collected from 10 geographically distinct fields across China (see detailed soil information in table S4). Salt stress in this experiment was applied with 300 mM NaCl.

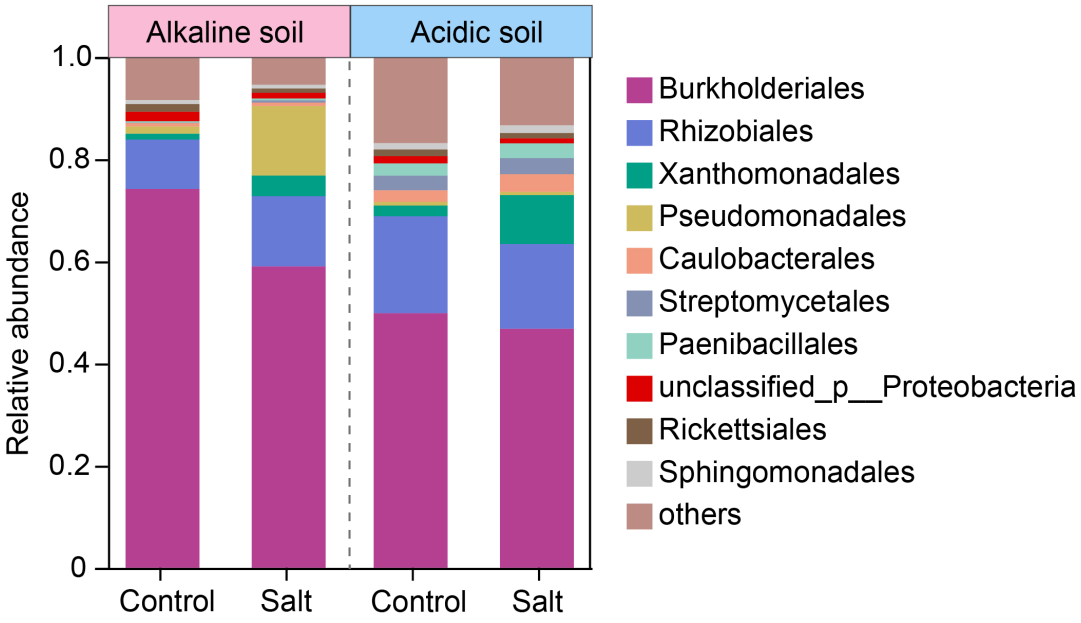

Fig. S3. The top 10 abundant bacterial orders of control and salt treatment for wild soybean growing in alkaline and acidic soils. Data are based on 16S rRNA gene barcoding. Salt stress in this experiment was applied with 300 mM NaCl (n = 3 to 5 biologically independent samples).

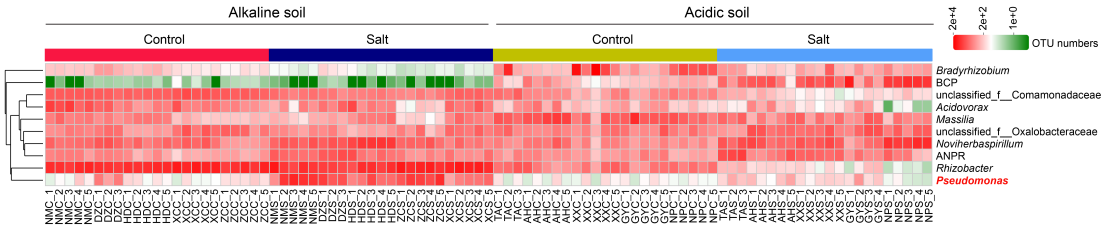

Fig. S4. The relative abundance of the top 10 bacterial genera of control and salt treatment for wild soybean growing in alkaline and acidic soils. *Pseudomonas* exhibited the most pronounced positive response to salt stress especially in alkaline soils. Salt stress in this experiment was applied with 300 mM NaCl. BCP: *Burkholderia-Caballeronia-Paraburkholderia*; ANPR: *Allorhizobium-Neorhizobium-Pararhizobium-Rhizobium*.

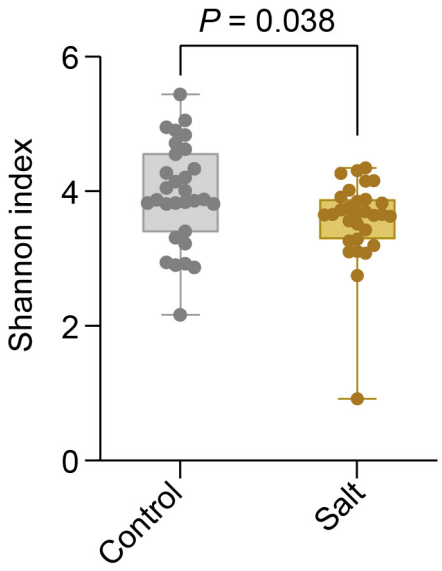

Fig. S5. Bacterial community alpha diversity (Shannon index) between control and salt stress for all plants. Tops and bottoms of boxes represent 25th and 75th percentiles, respectively. Horizontal bars within boxes denote medians, and the upper and lower whiskers represent the range of non-outlier data values. Statistical analysis was performed by two-sided Student's *t* test. Salt stress in this experiment was applied using 200 mM NaCl, as these crops have lower salt tolerance than wild soybean.

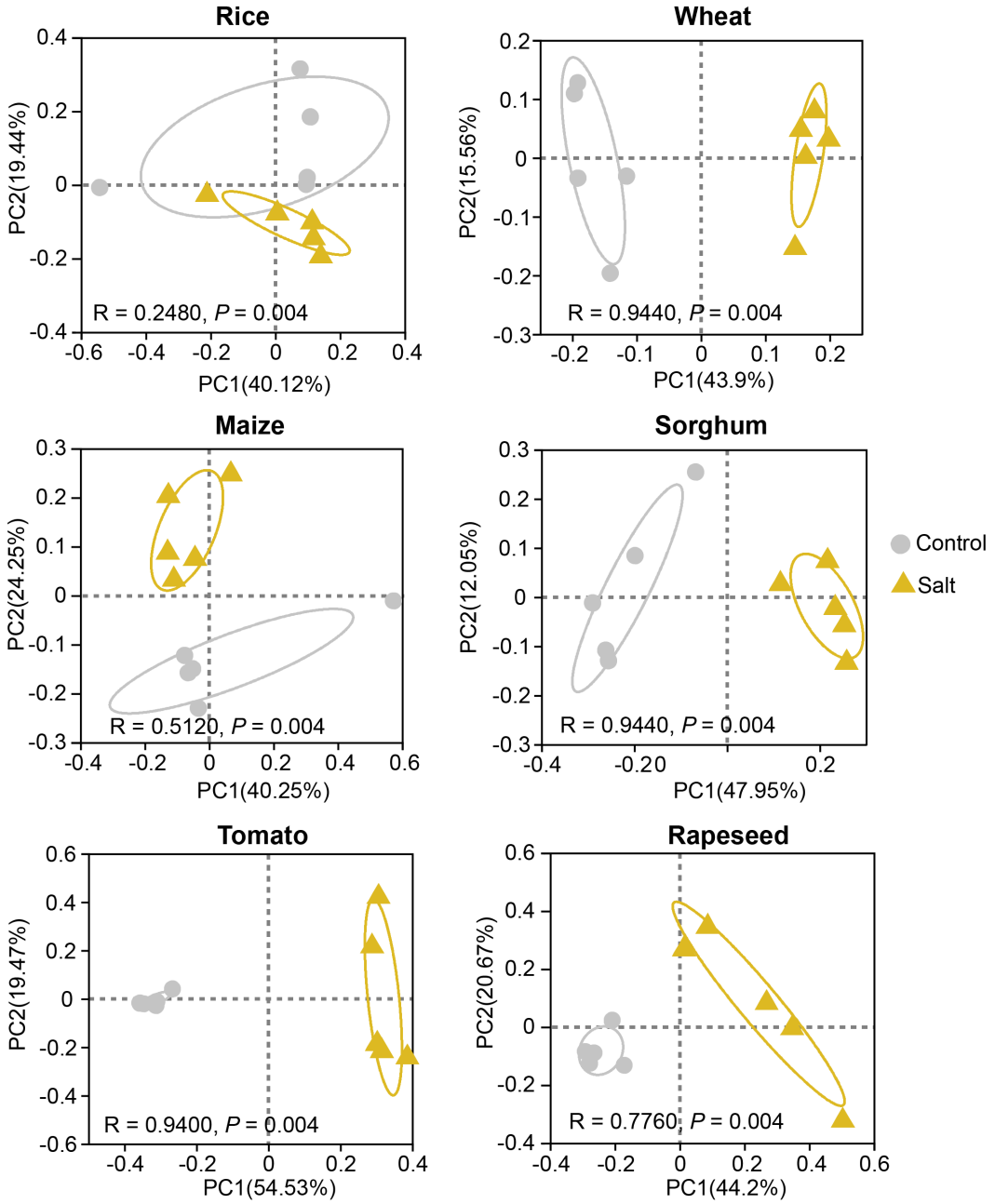

Fig. S6. PCoA ordination of the Bray-Curtis dissimilarity matrix (OTU level) between control and salt stress for each plant species. Statistical analysis was performed using ANOSIM (analysis of similarities). Salt stress in this experiment was applied using 200 mM NaCl, as these crops have lower salt tolerance than wild soybean.

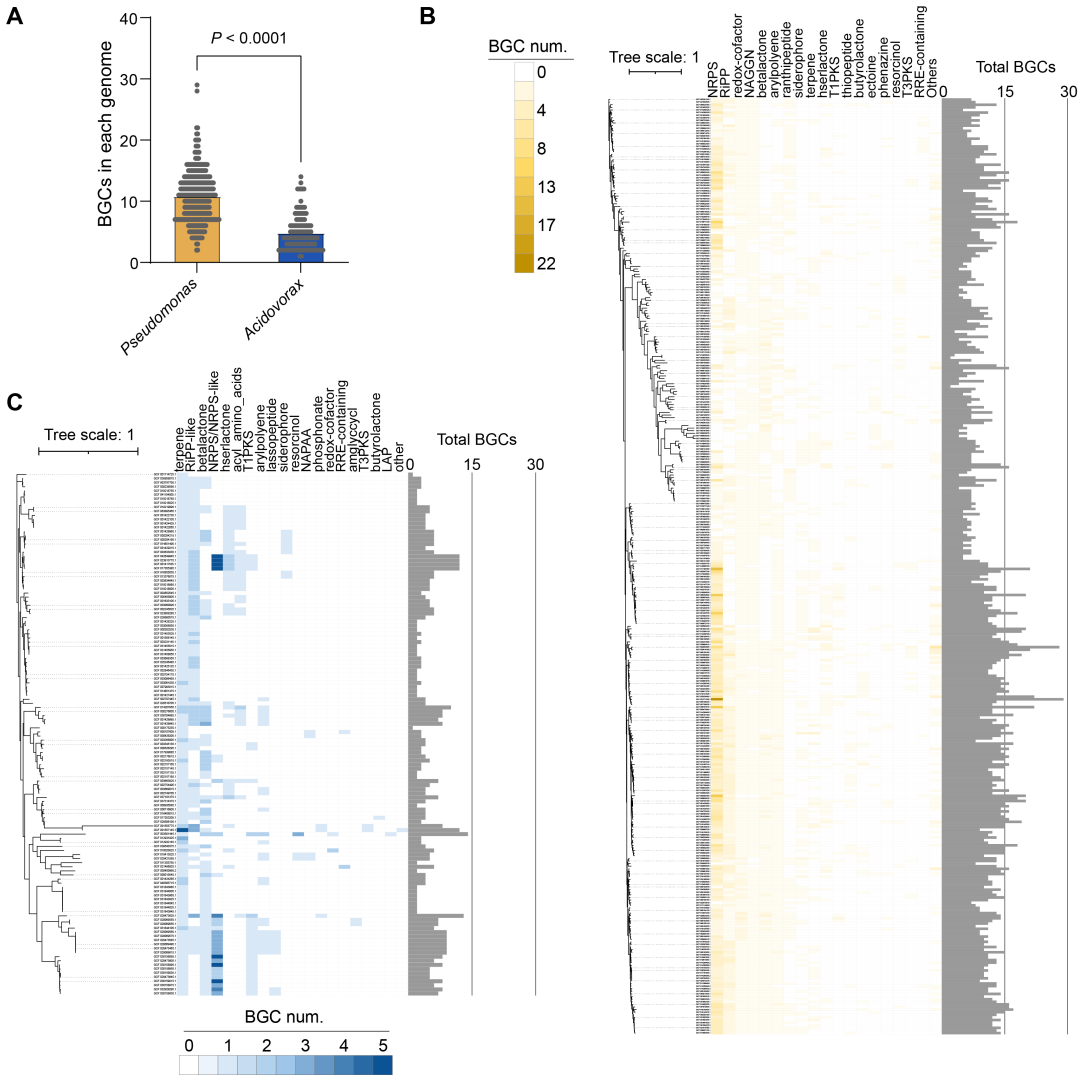

Fig. S7. Overview of biosynthetic gene clusters (BCGs) in *Pseudomonas* and *Acidovorax*. (**A**) Comparison of BGC numbers between *Pseudomonas* (n = 359) and *Acidovorax* (n = 128). Values are means ± SEM. Statistical analysis was performed by two-sided Student's t-test. (**B** and **C**) The maximum likelihood tree for *Pseudomonas* (B) and *Acidovorax* (C) genomes based on concatenation of 400 ubiquitously conserved proteins using PhyloPhlAn 3.0. Heatmap shows the number of various abundant BGCs and bar plot represents the total of BGCs in each genome.

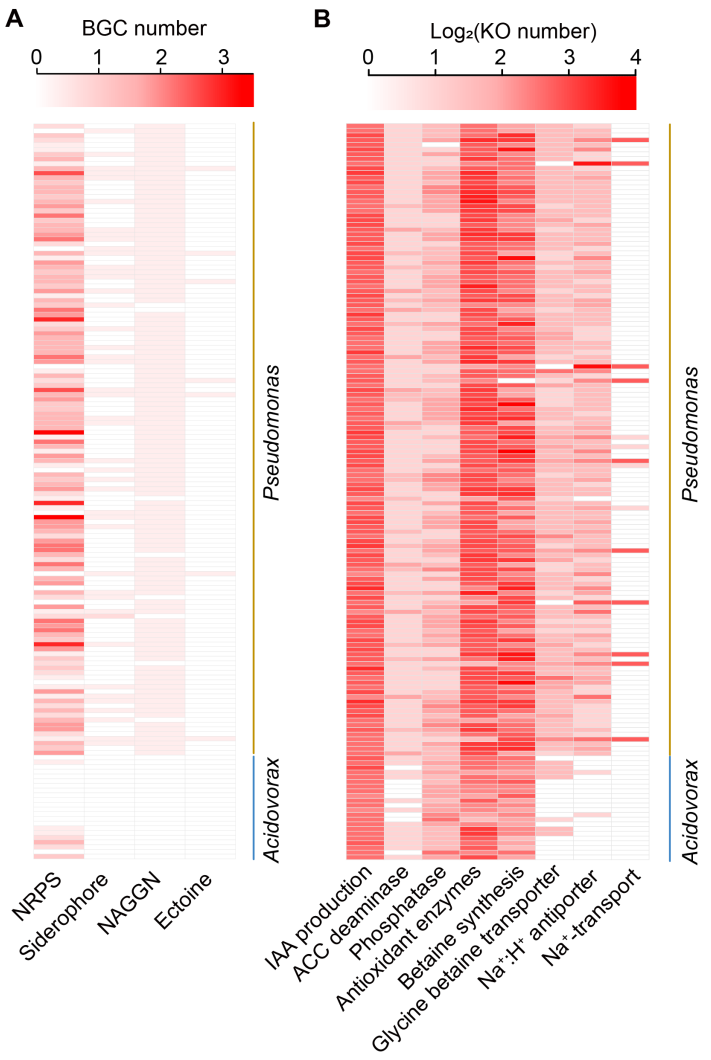

Fig. S8. Genetic potential for salt tolerance based on complete genome assemblies of *Pseudomonas* and *Acidovorax*. (**A**) The number of salt tolerance related BGCs in *Pseudomonas* and *Acidovorax* genomes. (**B**) The predicted genes associated with plant growth-promoting traits and salt stress alleviation in *Pseudomonas* and *Acidovorax* genomes.

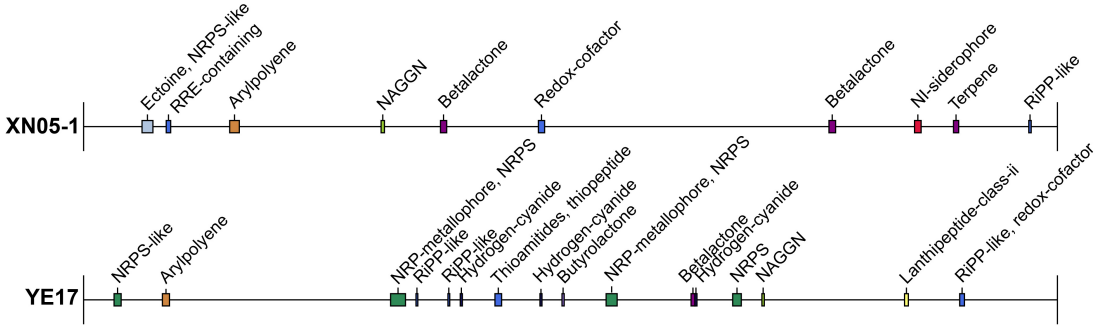

Fig. S9. Overview of BGCs in *Pseudomonas* strains XN05-1 and YE17. BGCs was predicted using the antiSMASH 7.1.0 online website (https://antismash.secondarymetabolites.org/). Both the strains harbored the NAGGN biosynthetic gene cluster.

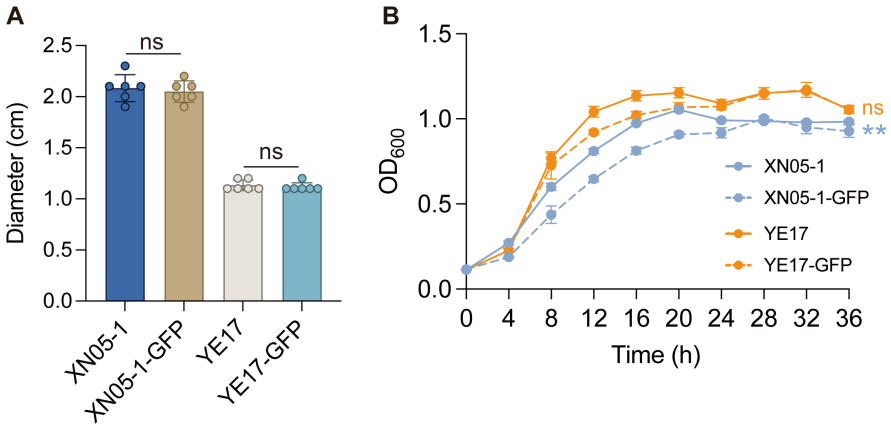

Fig. S10. Effects of green fluorescent protein (GFP) tagging on motility (a) and growth (b) in *Pseudomonas* strains XN05-1 and YE17. Wild-type strains: XN05-1 and YE17; GFP tagging strains: XN05-1-GFP and YE17-GFP. Statistical analysis was performed by two-sided Student's *t*-test.

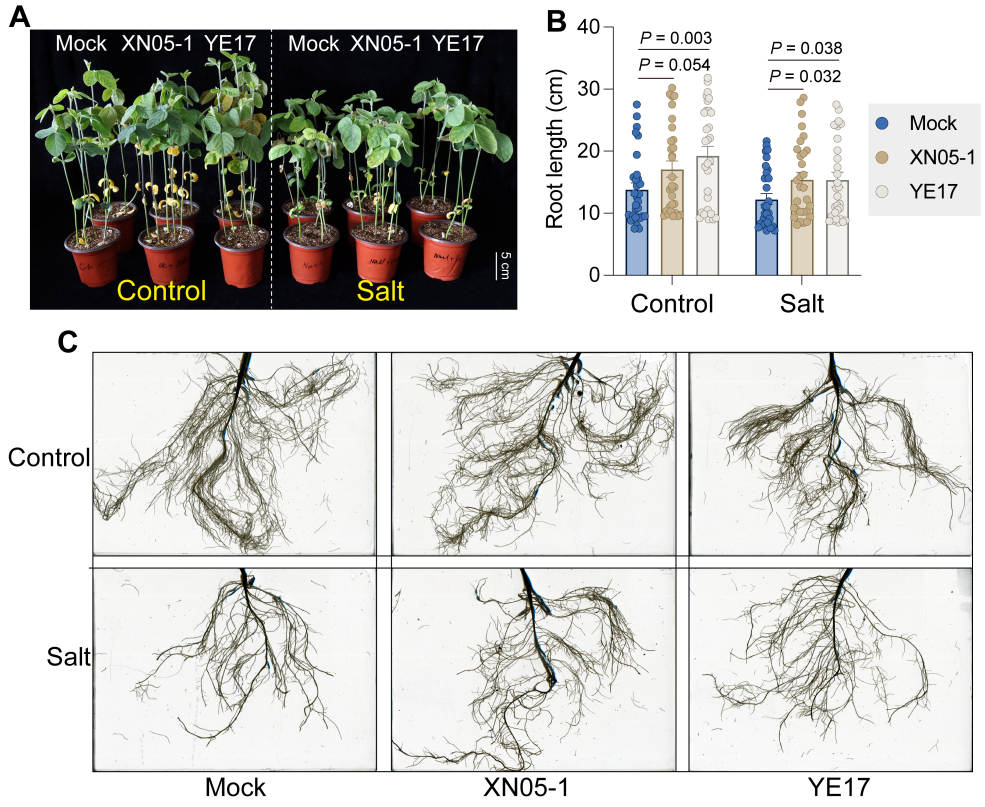

Fig. S11. Effects of *Pseudomonas* strains XN05-1 and YE17 on soybean growth and root development under salt stress. (**A**) Growth phenotype of soybean following inoculation with strains XN05-1 and YE17. Bars = 5 cm. (**B**) Primary root length. (**C**) Root system architecture. Statistical analysis was performed by two-tailed Student's *t*-test. The values represent the means ± SEM (n = 30 roots in Fig. B). Salt stress in this experiment was applied using 300 mM NaCl.

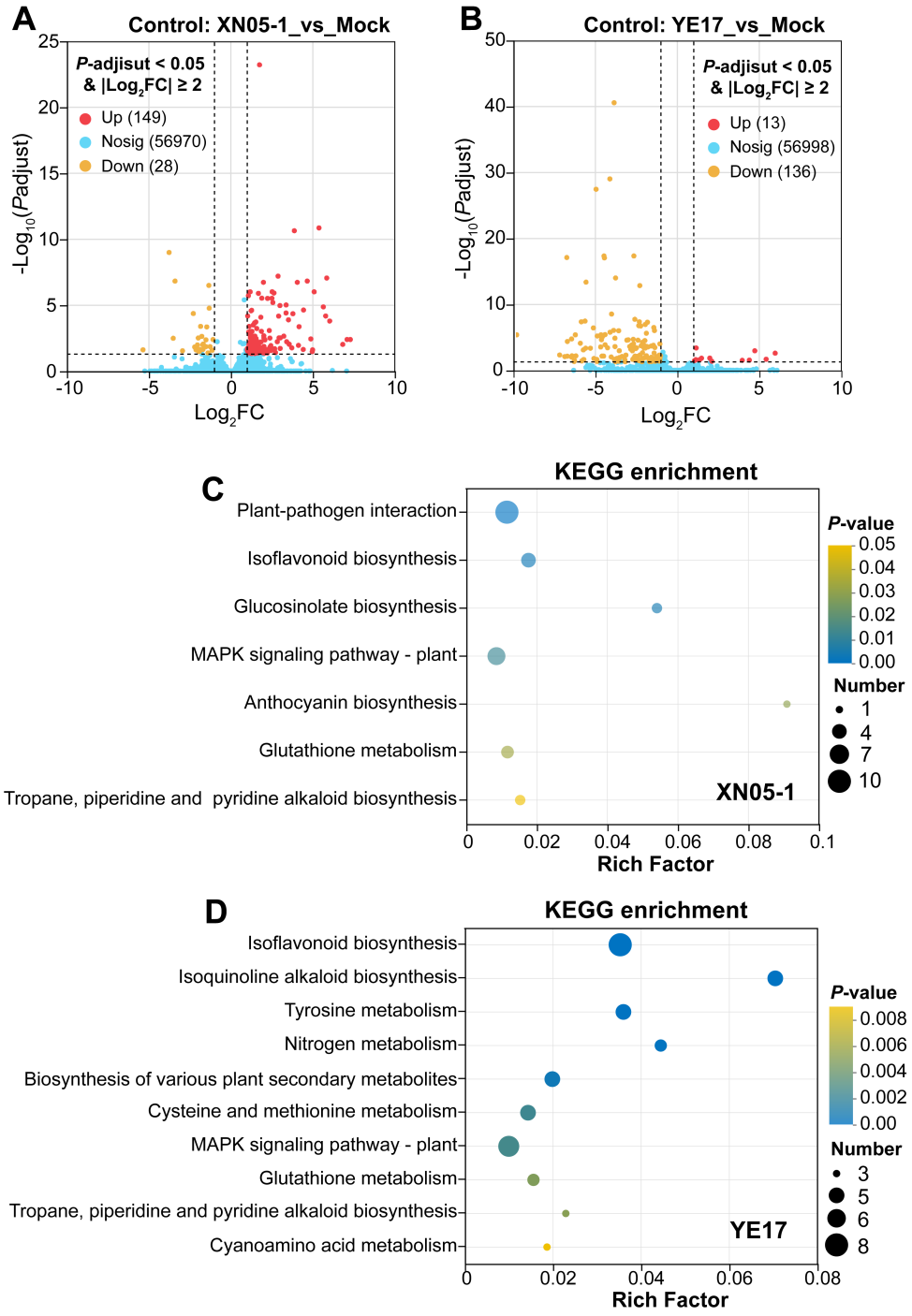

Fig. S12. Transcriptional responses of soybean roots to *Pseudomonas* strains XN05-1 and YE17 under non-saline conditions. (**A** and **B**) The volcano plot shows the differentially expressed genes induced by inoculation with strains XN05-1 and YE17. (**C** and **D**) KEGG enrichment analysis of differentially expressed genes in soybean root inoculated with XN05-1 and YE17 strains.

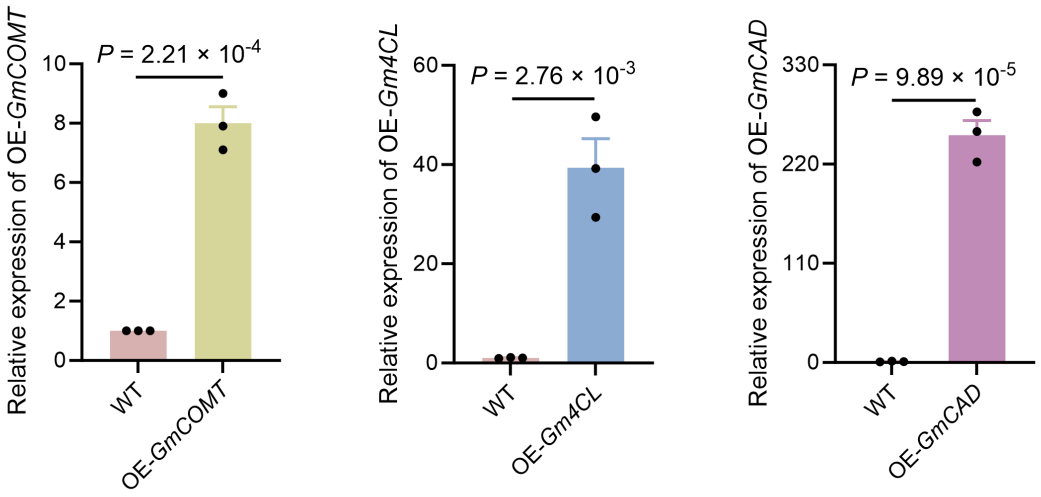

Fig. S13. The expression levels of *GmCAD*, *Gm4CL*, and *GmCOMT* in the corresponding overexpression lines. The values represent the means ± SEM (n = 3 roots). Statistical analysis was performed by two-tailed Student's t-test.

Supplementary Tables

Table S1. The information of 164 MAGs obtained in this study.

Table S2. COG functions of the enriched and depleted MAGs in salt-tressed rhizosphere soil of wild soybean.

Table S3. KO numbers of the enriched and depleted MAGs annotated to plant growth-promoting potential.

Table S4. The location and soil pH of each sample site.

Table S5. Summary of samples used for 16S rRNA gene barcoding analysis. Several treatments included less than five but more than three biological replicates due to the failure of DNA extraction or 16S rRNA gene PCR amplification.

Table S6. The salt tolerance of type strains within *Pseudomonas* and *Acidovorax* genera based on published literatures.

Table S7. The information of *Pseudomonas* genomes downloaded from NCBI database.

Table S8. The information of *Acidovorax* genomes downloaded from the NCBI database.

Table S9. Proteins encoded by NAGGN biosynthetic gene cluster in *Pseudomonas* strains XN05-1 and YE17.

Table S10. Differentially expressed genes (DEGs) induced by inoculation with *Pseudomonas* strains XN05-1 and YE17 under both control and salt stress conditions.

Table S11. An analysis of gene expression patterns associated with Na^+ transport.

Table S12. Primers used in this study.